Inorganic Chemistry

Article

pubs.acs.org/IC

Novel Stannatranes of the Type $N(CH_2CMe_2O)_3SnX$ (X = OR, SR, OC(O)R, $SP(S)Ph_2$, Halogen). Synthesis, Molecular Structures, and Electrochemical Properties

Thomas Zöller,[†] Christina Dietz,[†] Ljuba Iovkova-Berends,[†] Olga Karsten,[†] Gerrit Bradtmöller,[†] Ann-Kristin Wiegand,[†] Yu Wang,[‡] Viatcheslav Jouikov,[‡,*] and Klaus Jurkschat[†,*]

[†]Lehrstuhl für Anorganische Chemie II der Technischen Universität Dortmund, D-44221 Dortmund

[‡]UMR CNRS 6510, Molecular Chemistry and Photonics, University of Rennes, 35042 Rennes, France

Supporting Information

ABSTRACT: The syntheses of the stannatrane derivatives of the type $N(CH_2CMe_2O)_3SnX$ (**1**, X = O*t*-Bu; **2**, X = O*i*-Pr; **3**, X = 2,6-$Me_2C_6H_3O$; **4**, X = *p*-*t*-BuC_6H_4O; **5**, X = *p*-$NO_2C_6H_4O$; **6**, X = *p*-FC_6H_4O; **7**, X = *p*-$PPh_2C_6H_4O$; **8**, X = *p*-MeC_6H_4S; **9**, X = *o*-$NH_2C_6H_4O$; **10**, X = $OCPh_2CH_2NMe_2$; **11**, X = $Ph_2P(S)S$; **12**, X = *p*-*t*-$BuC_6H_4C(O)O$; **13**, X = Cl; **14**, X = Br; **15**, X = I; **16**, X = *p*-$N(CH_2CMe_2O)_3SnOSiMe_2C_6H_4SiMe_2O$) are reported. The compounds are characterized by X-ray diffraction analyses (**3**−**8**, **11**−**16**), multinuclear NMR spectroscopy, ^{13}C CP MAS (**14**) and ^{119}Sn CP MAS NMR (**13**, **14**) spectroscopy, mass spectrometry and osmometric molecular weight determination (**13**). Electrochemical measurements show that anodic oxidation of the stannatranes **4** and **8** occurs via electrochemically reversible electron transfer resulting in the corresponding cation radicals. The latter were detected by cyclic voltammetry (CV) and real-time electron paramagnetic resonance spectroscopy (EPR). DFT calculations were performed to compare the stannatranes **4**, **8**, and **13** with the corresponding cation radicals $\mathbf{4}^{+\bullet}$, $\mathbf{8}^{+\bullet}$, and $\mathbf{13}^{+\bullet}$, respectively.

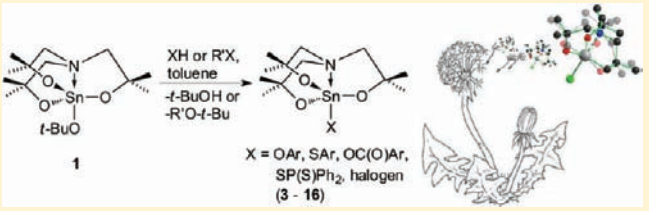

INTRODUCTION

Metal(IV)-derivatives of triethanolamines are called metallatranes.[1] These compounds are characterized by their cage structure, an intramolecular N → M (M = metal) interaction and chirality of the molecular framework which is described in terms of right- or left-handed (Δ or Λ) propeller geometry (Scheme 1).[2−4]

Scheme 1. Δ and Λ stereochemistry for metallatranes viewing along the Z−M−N axis (Z is omitted for clarity).

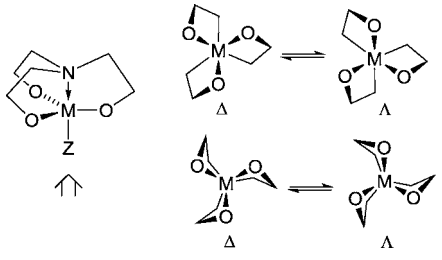

In the last decades the chemistry of metallatranes has been extensively studied and expanded across the periodic table.[5−11] Among the metallatranes especially group 14 element atranes are the most intensively studied representatives and have been reviewed in recent years.[9−11] Organostannatranes of the type $N(CH_2CR^1R^2O)_3SnR^3$ (R^1, R^2 = H, Me; R^3 = alkyl, aryl, CH_2SiMe_2R)[6,9,12−14] and stannatrane-like compounds of type $N[CH_2C(O)O]_3SnR^4$ (R^4 = alkyl, Ph, $CH_2CH_2CH_2NMe_2$, $CH_2CH_2CH_2N(O)Me_2$)[9] are also known for a long time but only four examples have been structurally characterized by single crystal X-ray diffraction analysis. The methylstannatrane, $[N(CH_2CH_2O)_3SnMe]_3\cdot 6H_2O$, (**A**), is a trimer via intermolecular Sn−O → Sn bridges[15] whereas, as result of steric protection respectively additional intramolecular N(O) → Sn coordination, the *t*-butyl-,[16] *o*-anisyl-,[12] and dimethylaminooxypropyl-substituted compounds $N(CH_2CH_2O)_3SnR$ (R = *t*-Bu, (**B**); *o*-$MeOC_6H_4$, (**C**)) and $N[CH_2C(O)O]_3Sn(CH_2)_3N(O)Me_2$[17] (**D**) are monomeric (Scheme 2).

Inorganic stannatranes that lack any tin−carbon bond are scarce[18−21] and to the best of our knowledge only three solid state structures of derivatives with nitrilotrisethanolato or nitrilotriacetate ligands have been reported (Scheme 3).[22−24]

In context with our ongoing studies on alkanol amin derivatives of tin,[25−27] the motivation for renewed research on inorganic stannatranes stems from the nontoxicity of these compounds because of the absence of any metal−carbon bond and the catalytic activity of alkanol amin derivatives of tin in polymerization reactions.[28]

Received: October 11, 2011
Published: December 23, 2011

Scheme 2. Monoorgano-stannatranes and stannatrane-like compounds.

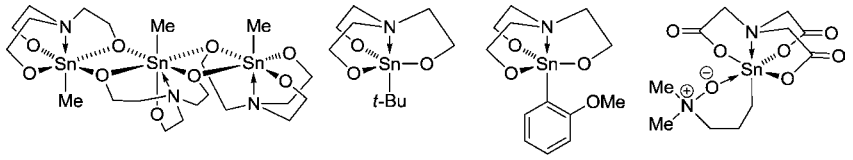

Scheme 3. Stannatranes and stannatrane-like compounds without Sn−C bonding.

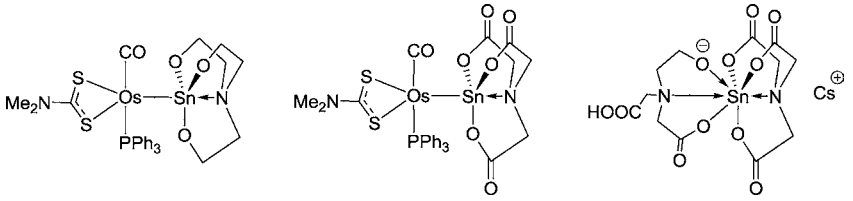

EXPERIMENTAL SECTION

General. All experimental manipulations were carried out under argon atmosphere using Schlenk technique. All solvents were purified by distillation under argon from appropriate drying agents according to standard procedures.[29] Tris(2-hydroxy-2-methylpropyl)amine, $N(CH_2CMe_2OH)_3$, and 2-(dimethylamino)-1,1-diphenylethanol, $Me_2NCH_2CPh_2OH$, were prepared from ammonia, dimethylamine, and 1,1-dimethyloxirane, respectively.[30] Tris(2-hydroxy-2-methylpropyl)-amine was recrystallized from dry diethyl ether before use. 1,4-Bis-(hydroxydimethylsilyl)benzene[31] and 4-(diphenylphosphino)phenol[32] were prepared according to literature methods.

The NMR spectra were recorded on Bruker DRX 500, Bruker DRX 400, and Bruker DPX 300 spectrometers. Chemical shifts δ are given in ppm and are referenced to the solvent peaks with the usual values calibrated against tetramethylsilane (^1H, ^{13}C, ^{29}Si), 80% H_3PO_4 (^{31}P), and tetramethylstannane (^{119}Sn).

The ^{119}Sn CP MAS NMR spectra were recorded with a BrukerAvance III 400 spectrometer using cross-polarization and high-power proton decoupling [conditions: 3.7 μs (90°) pulse, contact time 3 ms, 10 s recycle delay]. Spectra with different spinning rates between 5 and 9 kHz were recorded to unambiguously determine the isotropic chemical shifts. Tetracyclohexylstannane was used as secondary reference (δ = 97.35).

Elemental analyses were performed on a LECO CHNS-932 analyzer. No elemental analyses were performed for compounds **1** and **2** because of their extreme sensitivity toward hydrolysis. For compounds **6**, **10**, and **16** the experimentally determined values for carbon differ by 1−1.6% from the calculated ones. The electrospray mass spectra were recorded on a Thermoquest Finnigan instrument using CH_3CN or CH_2Cl_2 as a mobile phase.

*1-tert-Butanolato-2,8,9-trioxa-5-aza-3,3,7,7,10,10-hexamethyl-stannatricyclo-[3.3.3.0^{1,5}]undecane (**1**).* To a stirred solution of tin(IV)-*tert*-butoxide (4.21 g, 10.24 mmol) in dry toluene (350 mL) was added within 10 min at room temperature a solution of $N(CH_2CMe_2OH)_3$ (2.39 g, 10.24 mmol) in dry toluene (80 mL). After concentrating the mixture by azeotropic distillation the remaining solvent was removed under reduced pressure. Compound **1** (4.32 g, 10.24 mmol, quantitative) was obtained as colorless microcrystalline solid. ^1H NMR (300.13 MHz, C_6D_6, 298 K): δ 2.32 (s, $J(^1H-^{117/119}Sn)$ = 20.9 Hz, $^1J(^1H-^{13}C)$ = 137.1 Hz, 6H, NCH_2), 1.72 (s, $^1J(^1H-^{13}C)$ = 124.5 Hz, 9H, $C(CH_3)_3$), 1.22 (s, $^1J(^1H-^{13}C)$ = 125.6 Hz, 18H, $C(CH_3)_2$). $^{13}C\{^1H\}$ NMR (100.63 MHz, C_6D_6, 298 K): δ 70.4 (s, $J(^{13}C-^{117/119}Sn)$ = 48.4 Hz, NCH_2, $C(CH_3)_3$), 68.8 (s, $J(^{13}C-^{117/119}Sn)$ = 21.6 Hz, $C(CH_3)_2$), 33.7 (s, $^3J(^{13}C-^{117/119}Sn)$ = 27.5 Hz, $C(CH_3)_3$), 31.5 (s, $J(^{13}C-^{117/119}Sn)$ = 30.4 Hz, $C(CH_3)_2$). $^{119}Sn\{^1H\}$ NMR (111.89 MHz, $CDCl_3$, 298 K): δ −319 (s, $J(^{119}Sn-^{13}C)$ = 49 Hz, $J(^{119}Sn-^{13}C)$ = 30 Hz). mp 111−113 °C. IR (nujol, ν/cm^{-1}) = 2928, 2855, 1463, 1378, 1288, 1167, 1074, 978, 947, 921, 789, 725, 649. MS (ESI +): m/z = 216.2 $[C_{12}H_{26}NO_2]^+$, 234.2 $[N(CH_2CMe_2OH)_3 + H]^+$, 583.3 $[M - O^tBu + N(CH_2CMe_2OH)_3]^+$, 930.4 $[C_{36}H_{73}N_3O_9Sn_2 + H]^+$.

*1-iso-Propanolato-2,8,9-trioxa-5-aza-3,3,7,7,10,10-hexamethyl-stannatricyclo[3.3.3.0^{1,5}]undecane (**2**).* The procedure is the same as described for compound **1**, but $Sn(O\text{-}i\text{-}Pr)_4{\cdot}HO\text{-}i\text{-}Pr$ (1.17 g, 2.82 mmol) was used as starting material. Compound **2** (1.15 g, 2.82 mmol, quantitative) was obtained as colorless amorphous solid. ^1H NMR (500.13 MHz, C_6D_6, 298 K): δ 4.78 (complex pattern, 1H, OC*H*), 2.36 (s, 6H, NCH_2), 1.49 (complex pattern, 6H, $OCH(CH_3)_2$), 1.17 (s, $^1J(^1H-^{13}C)$ = 118.0 Hz, 18H, $C(CH_3)_2$). $^{13}C\{^1H\}$ NMR (100.63 MHz, C_6D_6, 298 K): δ 70.5 (s, $J(^{13}C-^{117/119}Sn)$ = 46.6 Hz, NCH_2), 68.8 (s, $J(^{13}C-^{117/119}Sn)$ = 17.5 Hz, $C(CH_3)_2$), 67.7 (s, $OCH(CH_3)_2$), 31.5 (s, $J(^{13}C-^{117/119}Sn)$ = 30.4 Hz, $C(CH_3)_2$), 28.0 (s, $^3J(^{13}C-^{117/119}Sn)$ = 27.5 Hz, $OCH(CH_3)_2$). $^{119}Sn\{^1H\}$ NMR (111.89 MHz, $CDCl_3$, 298 K): δ −312 (s, $J(^{119}Sn-^{13}C)$ = 52 Hz, $J(^{119}Sn-^{13}C)$ = 24 Hz). mp 97−98 °C. MS (ESI +): m/z = 162.2 $[HN(CH_2CMe_2OH)_2 + H]^+$, 234.2 $[N(CH_2CMe_2OH)_3 + H]^+$, 511.3 $[M - O\text{-}^i\text{Pr} + HN(CH_2CMe_2OH)_2]^+$, 583.3 $[M - O\text{-}^i\text{Pr} + N(CH_2CMe_2OH)_3]^+$, 930.4 $[C_{36}H_{73}N_3O_9Sn_2 + H]^+$, 1062.3 $[N(CH_2CMe_2O)_3SnOSn(OCMe_2CH_2)_3N + N(CH_2CMe_2O)_3Sn]^+$. IR (nujol, ν/cm^{-1}) = 2920, 2856, 1463, 1377, 1289, 1215, 1191, 1073, 977, 947, 788, 726, 649.

*1-(2,6-Dimethylphenolato)-2,8,9-trioxa-5-aza-3,3,7,7,10,10-hexamethyl-stannatricyclo[3.3.3.0^{1,5}]undecane (**3**).* To a stirred solution of **1** (1.29 g, 3.06 mmol) in dry toluene (200 mL) was added a toluene solution (50 mL) of 2,6-dimethylphenol (0.37 g, 3.03 mmol). The mixture was heated at reflux for 1.5 h and then concentrated by azeotropic distillation of *t*-BuOH/toluene. Slow cooling to room temperature provided a colorless amorphous solid. Recrystallization from toluene and subsequent washing with cold toluene gave colorless column-like crystals of **3** (1.32 g, 2.80 mmol, 92%). ^1H NMR (400.13 MHz, C_6D_6, 298 K): δ 7.07 (d, $^3J(^1H-^1H)$ = 7.4 Hz, 2H, *m*-H), 6.80 (t, $^3J(^1H-^1H)$ = 7.4 Hz, 1H, *p*-H), 2.71 (s, $^1J(^1H-^{13}C)$ = 126.2 Hz, 6H, *o*-(CH_3)), 2.23 (s, $J(^1H-^{117/119}Sn)$ = 21.3 Hz, $^1J(^1H-^{13}C)$ = 138.1 Hz, 6H, NCH_2), 1.09 (s, $^1J(^1H-^{13}C)$ = 125.8 Hz, 18H, $C(CH_3)_2$). $^{13}C\{^1H\}$ NMR (100.63 MHz, C_6D_6, 298 K): δ 157.9 (s, *i*-*C*), 129.4(s, *o*-*C*), 128.6 (s, *m*-*C*), 120.2 (s, *p*-*C*), 70.2 (s, $J(^{13}C-^{117/119}Sn)$ = 49.4 Hz, NCH_2), 69.3 (s, $J(^{13}C-^{117/119}Sn)$ = 21.1 Hz, $C(CH_3)_2$), 31.2 (s, $J(^{13}C-^{117/119}Sn)$ = 32.1 Hz, $C(CH_3)_2$), 18.0 (s, *o*-(CH_3)). $^{119}Sn\{^1H\}$ NMR (111.89 MHz, C_6D_6, 298 K): δ −333 (s). mp: 209−212 °C. Anal. Calcd. for $C_{20}H_{33}NO_4Sn$ (%): C 51.1, H 7.1, N 3.0. Found: C 51.1, H 7.1, N 2.9. MS (ESI+): m/z = 216.2 $[C_{12}H_{26}NO_2]^+$, 234.2 $[N(CH_2CMe_2OH)_3 + H]^+$, 350.1 $[M - OC_6H_3Me_2]^+$, 382.1 $[M - OC_6H_3Me_2 + MeOH]^+$, 583.3 $[M - OC_6H_3Me_2 + N(CH_2CMe_2OH)_3]^+$, 729.2 $[N(CH_2CMe_2O)_3SnOMe + N(CH_2CMe_2O)_3Sn]^+$, 930.5 $[C_{36}H_{73}N_3O_9Sn_2 + H]^+$.

*1-(4-tert-Butylphenolato)-2,8,9-trioxa-5-aza-3,3,7,7,10,10-hexamethyl-stannatricyclo[3.3.3.0^{1,5}]undecane (**4**).* The procedure is the same as described for compound **3**, with **1** (2.54 g, 6.02 mmol) and *p*-*tert*-butylphenol (0.90 g, 5.99 mmol) as starting materials.

dx.doi.org/10.1021/ic202179e | *Inorg. Chem.* 2012, 51, 1041−1056

Crystals of **4** (2.73 g, 5.48 mmol, 91%) were obtained as colorless columns. ^{1}H NMR (400.13 MHz, CD_2Cl_2, 298 K): δ 7.18 (d, $^3J(^1H-^1H)$ = 8.7 Hz, 2H, *m*-H), 6.85 (d, $^3J(^1H-^1H)$ = 8.7 Hz, 2H, *o*-H), 2.96 (s, $J(^1H-^{117/119}Sn)$ = 23.3 Hz, $^1J(^1H-^{13}C)$ = 138.7 Hz, 6H, NCH_2), 1.33 (s, $^1J(^1H-^{13}C)$ = 126.0 Hz, 18H, $C(CH_3)_2$), 1.28 (s, $^1J(^1H-^{13}C)$ = 125.4 Hz, 9H, $C(CH_3)_3$). $^{13}C\{^1H\}$ NMR (100.63 MHz, CD_2Cl_2, 298 K): δ 158.0 (s, *ipso*-C), 142.0 (s, *p*-C), 126.3 (s, *m*-C), 118.4 (s, *o*-C), 70.5 (s, $J(^{13}C-^{117/119}Sn)$ = 49.5 Hz, NCH_2), 68.8 (s, $J(^{13}C-^{117/119}Sn)$ = 19.1 Hz, $C(CH_3)_2$), 34.1 (s, $C(CH_3)_3$), 31.6 (s, $C(CH_3)_3$), 31.2 (s, $J(^{13}C-^{117/119}Sn)$ = 31.1 Hz, $C(CH_3)_2$). $^{119}Sn\{^1H\}$ NMR (111.89 MHz, C_6D_6, 298 K): δ −322 (s). Anal. Calcd. for $C_{22}H_{37}NO_4Sn$ (%): C 53.0, H 7.5, N 2.8. Found: C 53.0, H 7.5, N 2.7. MS (ESI +): *m*/*z* = 216.2 $[C_{12}H_{26}NO_2]^+$, 234.2 $[N(CH_2CMe_2OH)_3 + H]^+$, 350.1 $[M - OC_6H_4$-^{t}Bu$]^+$, 382.1 $[M - OC_6H_4$-^{t}Bu + MeOH$]^+$, 583.3 $[M - OC_6H_4$-^{t}Bu + $N(CH_2CMe_2OH)_3]^+$.

1-(4-Nitrophenolato)-2,8,9-trioxa-5-aza-3,3,7,7,10,10-hexamethyl-stannatricyclo[3.3.3.0^{1,5}]undecane (**5**). The procedure is the same as described for compound **3**, with **1** (1.61 g, 3.81 mmol) and 4-nitrophenol (0.53 g, 3.81 mmol) as starting materials. Recrystallization from toluene gave compound **5**, as its toluene solvate **5**·0.25C_7H_8 (1,74 g, 3.41 mmol, 90%), as yellowish columns. ^{1}H NMR (300.13 MHz, CD_2Cl_2, 300 K): δ 8.07 (d, $^3J(^1H-^1H)$ = 9.2 Hz, 2H, *m*-*H*), 7.26−7.12 (m, toluene), 7.01 (d, $^3J(^1H-^1H)$ = 8.5 Hz, 2H, *o*-*H*), 3.00 (s, $J(^1H-^{117/119}Sn)$ = 23.3 Hz, $^1J(^1H-^{13}C)$ = 139.2 Hz, 6H, NCH_2), 2.12 (s, toluene), 1.34 (s, $^1J(^1H-^{13}C)$ = 126.0 Hz, 18H, $C(CH_3)_2$). $^{13}C\{^1H\}$ NMR (100.63 MHz, CD_2Cl_2, 300 K): δ 166.8 (s, *ipso*-C), 140.3 (s, *p*-C), 138.1 (toluene), 129.1 (toluene), 128.4 (toluene), 126.0 (s, *m*-C), 125.5 (toluene), 119.1 (s, *o*-C), 70.5 (s, $J(^{13}C-^{117/119}Sn)$ = 18.9 Hz, $C(CH_3)_2$), 70.2 (s, $J(^{13}C-^{117/119}Sn)$ = 50.6 Hz, NCH_2), 31.1 (s, $J(^{13}C-^{117/119}Sn)$ = 31.8 Hz, $C(CH_3)_2$), 21.4 (toluene). $^{119}Sn\{^1H\}$ NMR (111.89 MHz, C_6D_6, 295 K): δ −315 (s). mp = 114−117 °C. Anal. Calcd for $C_{18}H_{28}N_2O_6Sn$·0.25 C_7H_8 (%): C 46.5, H 5.9, N 5.5. Found: C 46.3, H 5.9, N 5.2. (ESI+): *m*/*z* = 216.3 $[C_{12}H_{26}NO_2]^+$, 234.3 $[N(CH_2CMe_2OH)_3 + H]^+$, 350.1 $[M - OC_6H_4NO_2]^+$, 583.3 $[M - OC_6H_4NO_2 + N(CH_2CMe_2OH)_3]^+$, 715.3 $[N(CH_2CMe_2O)_3$-$SnOSn(OCMe_2CH_2)_3N + H]^+$, 729.3 $[N(CH_2CMe_2O)_3SnOMe + N(CH_2CMe_2O)_3Sn]^+$, 930.5 $[C_{36}H_{73}N_3O_9Sn_2 + H]^+$, 1062.4 $[N(CH_2CMe_2O)_3SnOSn(OCMe_2CH_2)_3N + N(CH_2CMe_2O)_3Sn]^+$.

1-(4-Fluorophenolato)-2,8,9-trioxa-5-aza-3,3,7,7,10,10-hexamethyl-stannatricyclo[3.3.3.0^{1,5}]undecane (**6**). The procedure is the same as described for compound **3**, with **1** (1.56 g, 3.70 mmol) and 4-fluorophenol (0.41 g, 3.66 mmol) as starting materials. Crystals of compound **6** (1.10 g, 2.39 mmol, 65%) were obtained as colorless blocks. ^{1}H NMR (300.13 MHz, CD_2Cl_2): δ 6.94−6.80 (m, 4H, *aryl*-*H*), 2.96 (s, $J(^1H-^{117/119}Sn)$ = 23.5 Hz, $^1J(^1H-^{13}C)$ = 139.1 Hz, 6H, NCH_2), 1.32 (s, $^1J(^1H-^{13}C)$ = 126.2 Hz, 18H, $C(CH_3)_2$). $^{13}C\{^1H\}$-NMR (100.63 MHz, CD_2Cl_2): δ 156.6 (d, $^1J(^{13}C-^{19}F)$ = 234.8 Hz, *ipso*-C), 156.6 (s, *o*-C), 119.8 (d, $^3J(^{13}C-^{19}F)$ = 7.9 Hz, *m*-C), 115.5 (d, $^2J(^{13}C-^{19}F)$ = 22.7 Hz, *p*-C), 70.4 (s, $J(^{13}C-^{119}Sn)$ = 49.4 Hz, NCH_2), 70.0 (s, $J(^{13}C-^{119}Sn)$ = 18.7 Hz, $C(CH_3)_2$), 31.2 (s, $^3J(^{13}C-^{119}Sn)$ = 31.1 Hz, $C(CH_3)_2$). $^{119}Sn\{^1H\}$ NMR (111.89 MHz, CD_2Cl_2): δ −313. mp: 197−198 °C. Anal. Calcd for $C_{18}H_{28}FNO_4Sn$ (%): C 47.0, H 6.1, N 3.0. Found: C 45.8, H 6.1, N 2.8. MS (ESI+): *m*/*z* = 234.3 $[N(CH_2CMe_2OH)_3 + H]^+$, 391.2 $[M - OC_6H_4F + MeCN]^+$, 583.3 $[M - OC_6H_4F + N(CH_2CMe_2OH)_3]^+$, 715.3 $[N(CH_2CMe_2O)_3SnOSn(OCMe_2CH_2)_3N + H]^+$. MS (ESI−): *m*/*z* = 91.0, 137.0.

1-(4-Diphenylphosphinophenolato)-2,8,9-trioxa-5-aza-3,3,7,7,10,10-hexamethyl-stannatricyclo[3.3.3.0^{1,5}]undecane (**7**). The procedure is the same as described for compound **3**, with **1** (0.94 g, 2.23 mmol) and 4-(diphenylphosphino)phenol (0.62 g, 2.23 mmol) as starting materials. Crystallization from toluene and subsequent washing with cold toluene gave **7** (1.23 g, 1.96 mmol, 88%) as colorless plates. ^{1}H NMR (300.13 MHz, CD_2Cl_2, 296 K): δ 7.38−7.24 (m, 10H, *aryl*-*H*), 7.20−7.12 (m, 2H, *aryl*-*H*), 6.98−6.92 (m, 2H, *aryl*-*H*), 2.97 (s, $J(^1H-^{117/119}Sn)$ = 23.4 Hz, $^1J(^1H-^{13}C)$ = 138.8 Hz, 6H, NCH_2), 1.33 (s, $^1J(^1H-^{13}C)$ = 126.1 Hz, 18H, $C(CH_3)_2$). $^{13}C\{^1H\}$ NMR (75.48 MHz, CD_2Cl_2, 296 K): δ 161.7 (s, *aryl*-*C*), 138.8 (d, $J(^{13}C-^{31}P)$ = 11.3 Hz, *aryl*-*C*), 135.9 (d, $J(^{13}C-^{31}P)$ = 21.8 Hz, *aryl*-*C*), 133.5 (d, $J(^{13}C-^{31}P)$ = 19.1 Hz, *aryl*-*C*), 128.6 (d, $J(^{13}C-^{31}P)$ = 8.9 Hz, *aryl*-*C*), 128.5 (s, *aryl*-*C*), 125.6 (d, $J(^{13}C-^{31}P)$ = 7.3 Hz, *aryl*-*C*), 119.5 (d, $J(^{13}C-^{31}P)$ = 8.3 Hz, *aryl*-*C*), 70.4 (s, $J(^{13}C-^{117/119}Sn)$ = 50.0 Hz, NCH_2), 70.1 (s, $J(^{13}C-^{117/119}Sn)$ = 19.1 Hz, $C(CH_3)_2$), 31.2 (s, $J(^{13}C-^{117/119}Sn)$ = 27.5 Hz, $C(CH_3)_2$). $^{31}P\{^1H\}$ NMR (121.50 MHz, CD_2Cl_2, 296 K): δ−6.3 (s, $J(^{31}P-^{13}C)$ = 19.2 Hz). $^{119}Sn\{^1H\}$ NMR (111.89 MHz, CD_2Cl_2, 296 K): δ −311 (s). mp = 217−219 °C. Anal. Calcd for $C_{29}H_{36}NO_4PSn$ (%): C 57.5, H 6.1, N 2.2. Found: C 57.5, H 6.1, N 1.9. (ESI+): *m*/*z* = 216.2 $[C_{12}H_{26}NO_2]^+$, 234.3 $[N(CH_2$-$CMe_2OH)_3 + H]^+$, 279.1 $[Ph_2PC_6H_4OH + H]^+$, 583.3 $[M - OC_6H_4NO_2 + N(CH_2CMe_2OH)_3]^+$.

1-(4-Methylthiophenolato)-2,8,9-trioxa-5-aza-3,3,7,7,10,10-hexamethyl-stannatricyclo[3.3.3.0^{1,5}]undecane (**8**). The procedure is the same as described for compound **3**, with **1** (1.79 g, 4.24 mmol) and *p*-methylthiophenol (0.53 g, 4.27 mmol) as starting materials. Crystallization from toluene/hexane and subsequent washing with hexane gave **8** (1.72 g, 3.64 mmol, 86%) as colorless columns. ^{1}H NMR (400.13 MHz,C_6D_6, 298 K): δ 7.91 (d, $^3J(^1H-^1H)$ = 8.0 Hz, $^1J(^1H-^{13}C)$ = 160.8 Hz, 2H, *o*-*H*), 6.80 (d, $^3J(^1H-^1H)$ = 8.0 Hz, $^1J(^1H-^{13}C)$ = 158.3 Hz, 2H, *m*-*H*), 2.26 (s, $J(^1H-^{117/119}Sn)$ = 21.0 Hz, 6H, NCH_2), 1.93 (s, 3H, $C_6H_4-CH_3$), 1.12 (s, $^1J(^1H-^{13}C)$ = 125.7 Hz, 18H, CCH_3). $^{13}C\{^1H\}$ NMR (100.63 MHz, C_6D_6, 298 K): δ 136.2 (s, *p*-C), 135.6 (s, *i*-C), 135.0 (s, $^4J(^{13}C-^{117/119}Sn)$ = 30.3 Hz, *o*-C), 118.4 (s, $^5J(^{13}C-^{117/119}Sn)$ = 9.5 Hz, *m*-C), 70.6 (s, $J(^{13}C-^{117/119}Sn)$ = 48.0 Hz, NCH_2), 69.5 (s, $J(^{13}C-^{117/119}Sn)$ = 30.6 Hz, $C(CH_3)_2$), 31.3 (s, $J(^{13}C-^{117/119}Sn)$ = 27.5 Hz, $C(CH_3)_2$), 20.9 (s, C_6H_4-CH_3) . $^{119}Sn\{^1H\}$ NMR (111.89 MHz, C_6D_6, 298 K): δ −227 (s, $J(^{119}Sn-^{13}C)$ = 29 Hz, $J(^{119}Sn-^{13}C)$ = 48 Hz). mp: 124−126 °C. Anal. Calcd for $C_{19}H_{31}NO_3SSn$ (%): C 48.3, H 6.6, N 3.0. Found: C 48.3, H 6.5, N 2.8. MS (ESI +): *m*/*z* = 216.2 $[C_{12}H_{26}NO_2]^+$, 234.2 $[N(CH_2CMe_2OH)_3 + H]^+$, 391.2 $[M - SC_6H_4Me + MeCN]^+$, 474.1 $[M + H]^+$, 496.1 $[M + Na]^+$.

1-(2-Aminophenolato)-2,8,9-trioxa-5-aza-3,3,7,7,10,10-hexamethylstannatricyclo[3.3.3.0^{1,5}]undecane (**9**). The procedure is the same as described for compound **3** with **1** (1.48 g, 3.51 mmol) and 2-aminophenol (0.38 g, 3.48 mmol) as starting materials. Compound **9** (1.60 g, 3.48 mmol, 99%) was obtained as colorless solid. ^{1}H NMR (300.13 MHz, CD_2Cl_2): δ 7.08−7.04 (complex pattern, 2H, H_4, H_6), 6.94−6.91 (complex pattern, 1H, H_5), 6.62 (dt, $^3J(^1H-^1H)$ = 1.4 Hz, $^4J(^1H-^1H)$ = 7.5 Hz 1H, H_3), 3.93 (s, broad, 2H, NH_2), 2.87 (s, $J(^1H-^{117/119}Sn)$ = 19.3 Hz, 6H, NCH_2), 1.27 (s, $^1J(^1H-^{13}C)$ = 125.5 Hz, 18H, $C(CH_3)_2$). $^{13}C\{^1H\}$ NMR (100.63 MHz, CD_2Cl_2): δ 157.1 (s, C_1), 129.2 (s, C_2), 128.4 (s, C_4), 125.3 (s, C_5), 117.6 (s, C_6), 117.0 (s, C_3), 70.9 (s, $J(^{13}C-^{117/119}Sn)$ = 50.3 Hz, NCH_2), 68.5 (s, $J(^{13}C-^{117/119}Sn)$ = 22.8 Hz, $C(CH_3)_2$,), 31.5 (s, $J(^{13}C-^{117/119}Sn)$ = 33.0 Hz, $C(CH_3)_2$). $^{119}Sn\{^1H\}$ NMR (111.89 MHz, CD_2Cl_2): δ −432 (s). mp: 198−200 °C (decomposition). Anal. Calcd. for $C_{18}H_{30}N_2O_4$-Sn (%): C 47.3, H 6.6, N 6.1. Found: C 47.6, H 6.5, N 5.4. MS (ESI+): *m*/*z* = 216.3 $[C_{12}H_{26}NO_2]^+$, 234.3 $[N(CH_2CMe_2OH)_3 + H]^+$, 391.2 $[M - OC_6H_4NH_2 + MeCN]^+$, 459.2 $[M + H]^+$, 583.4 $[M - OC_6H_4NH_2 + N(CH_2CMe_2OH)_3]^+$, 715.3 $[N(CH_2CMe_2O)_3SnOSn$-$(OCMe_2CH_2)_3N + H]^+$, 806.4 $[M + C_{12}H_{24}NO_3Sn]^+$.

1-(N,N-Dimethyl-2,2-diphenyl-aminoethanolato)-2,8,9-trioxa-5-aza-3,3,7,7,10,10-hexamethyl-stannatricyclo[3.3.3.0^{1,5}]undecane (**10**). The procedure is the same as described for compound **3**, with **1** (1.49 g, 3.53 mmol) and 2-(dimethylamino)-1,1-diphenylethanol (0.85 g, 3.52 mmol) as starting materials. After removing the volatiles under reduced pressure, compound **10** (1.99 g, 3.37 mmol, 95%) was obtained as yellowish oil that solidified upon standing. ^{1}H NMR (500.13 MHz, C_6D_6, 303 K): δ 8.18 (d, $^3J(^1H-^1H)$ = 7.3 Hz, 4H, *aryl*-*H*), 7.40−7.36 (m, 6H, *aryl*-*H*), 3.48 (s, $J(^1H-^{117/119}Sn)$ = 25.3 Hz, 2H, Me_2NCH_2) 2.63 (s, $J(^1H-^{117/119}Sn)$ = 16.1 Hz, 6H, NCH_2), 2.43 (s, $J(^1H-^{117/119}Sn)$ = 12.2 Hz, 6H, $N(CH_3)_2$), 1.48 (s, 18H, $C(CH_3)_2$). $^{13}C\{^1H\}$ NMR (100.63 MHz, CD_2Cl_2, 298 K): δ 152.0 (s, $^3J(^{13}C-^{117/119}Sn)$ = 27.8 Hz, *i*-C), 127.9, 126.4, 126.0 (s, *aryl*-C), 73.3 (s, $J(^{13}C-^{117/119}Sn)$ = 25.5 Hz, CPh_2O), 70.6 (s, $J(^{13}C-^{117/119}Sn)$ = 50.1 Hz, NCH_2), 68.2 (s, Me_2NCH_2), 67.9 (s, $J(^{13}C-^{117/119}Sn)$ = 27.6 Hz, $C(CH_3)_2O$), 47.3 (s, $N(CH_3)_2$), 32.2 (s, $J(^{13}C-^{117/119}Sn)$ = 32.6 Hz, $C(CH_3)_2$). $^{119}Sn\{^1H\}$ NMR (111.89 MHz, C_6D_6, 303 K): δ −462 ($J(^{119}Sn-^{13}C)$ = 29 Hz, $J(^{119}Sn-^{13}C)$ = 50 Hz). mp: 130−132 °C. Anal. Calcd. for $C_{28}H_{42}N_2O_4Sn$ (%): C 57.1, H 7.2, N 4.8. Found: C

dx.doi.org/10.1021/ic202179e | *Inorg. Chem.* 2012, 51, 1041−1056

55.5, H 6.9, N 4.4. MS (ESI +): m/z = 224.2 $[Me_2NCH_2CPh_2]^+$, 242.2 $[Me_2NCH_2CPh_2OH + H]^+$, 583.4 $[M - OCPh_2CH_2NMe_2 + N(CH_2CMe_2OH)_3]^+$, 591.3 $[M + H]^+$, 715.2 $[N(CH_2CMe_2O)_3SnOSn(OCMe_2CH_2)_3N + H]^+$, 930.4 $[C_{36}H_{73}N_3O_9Sn_2 + H]^+$, 954.4, 1062.4 $[N(CH_2CMe_2O)_3SnOSn(OCMe_2CH_2)_3N + N(CH_2CMe_2O)_3Sn]^+$, 1256.3.

*1-Diphenyldithiophosphinato 2,8,9-trioxa-5-aza-3,3,7,7,10,10-hexamethyl-stannatricyclo[3.3.3.0^{1,5}]undecane (**11**).* To a magnetically stirred solution of **1** (0.58 g, 1.37 mmol) in dry toluene (70 mL) a solution of diphenylphosphinodithioic acid (0.34 g, 1.36 mmol) in dry toluene (40 mL) was added dropwise at room temperature. After stirring for 18 h the volatiles were removed under reduced pressure. The residue was dissolved in dry toluene (10 mL), heated to reflux and filtered. Cooling of the filtrate to room temperature and standing for several days gave **11** (0.70 g, 1.17 mmol, 85%) as colorless crystals. ^{1}H NMR (400.13 MHz, C_6D_6, 298 K): δ 8.23 (ddd, $^3J(^1H-^{31}P)$ = 14.5 Hz, $^3J(^1H-^1H)$ = 3.2 Hz, $^3J(^1H-^1H)$ = 2.5 Hz, 4H, *m-H*), 7.08 (m, 6H, *o*-H, *p-H*), 2.55 (s, $J(^1H-^{117/119}Sn)$ = 20.7, 6H, NCH_2), 1.21 (s, $^1J(^1H-^{13}C)$ = 125.2 Hz, 18H, $C(CH_3)_2$). $^{13}C\{^1H\}$ NMR (100.63 MHz, C_6D_6, 298 K): δ 139.4 (d, $^1J(^{13}C-^{31}P)$ = 85.2 Hz, $^3J(^{13}C-^{117/119}Sn)$ = 16.2 Hz), *i-C*), 131.7 (d, $^2J(^{13}C-^{31}P)$ = 11.7 Hz, *o-C*), 130.8 (d, $^4J(^{13}C-^{31}P)$ = 3.0 Hz, *p-C*), 128.0 (d, $^3J(^{13}C-^{31}P)$ = 13.0 Hz, *m-C*), 70.6 (s, $J(^{13}C-^{117/119}Sn)$ = 31.0 Hz, $C(CH_3)_2O$), 70.3 (s, $J(^{13}C-^{117/119}Sn)$ = 51.3 Hz, NCH_2), 31.5 (s, $J(^{13}C-^{117/119}Sn)$ = 31.7 Hz, $C(CH_3)_2$). $^{31}P\{^1H\}$ NMR (81.02 MHz, C_6D_6, 298 K): δ 56.5 (s, $^2J(^{31}P-^{119}Sn)$ = 63.0 Hz, $^2J(^{31}P-^{117}Sn)$ = 61.0 Hz, $^1J(^{31}P-^{13}C)$ = 85.2 Hz, $^2J(^{31}P-^{13}C)$ = 11.9 Hz). $^{119}Sn\{^1H\}$ NMR (112 MHz, C_6D_6, 298 K): δ −246 (d, $^2J(^{119}Sn-^{31}P)$ = 64 Hz). Mp. 180−182 °C (decomposition). Anal. Calcd. for $C_{24}H_{34}NO_3PS_2Sn$ (%): C 48.2, H 5.7, N 2.3. Found: C 48.4, H 5.7, N 2.2. MS (ESI +): m/z = 234.3 $[N(CH_2CMe_2OH)_3 + H]^+$, 391.1 $[M - SP(S)Ph_2 + MeCN]^+$, 583.3 $[M - SP(S)Ph_2 + N(CH_2CMe_2OH)_3]^+$, 600.2 $[M + H]^+$. MS (ESI$^-$): m/z = 248.9 $[SP(S)Ph_2]^-$.

*1-(4-tert-Butylbenzoato 2,8,9-trioxa-5-aza-3,3,7,7,10,10-hexamethyl-stannatricyclo[3.3.3.0^{1,5}]undecane (**12**).* The procedure is the same as described for compound **11**, with **1** (1.66 g, 3.93 mmol) and 4-*tert*-butylbenzoic acid (0.70 g, 3.93 mmol) as starting materials. Compound **12** was obtained as colorless amorphous solid (2.07 g, 3.93 mmol, quantitative). Recrystallization from toluene/hexane gave crystals suitable for single crystal X-ray diffraction analysis. ^{1}H NMR (400.13 MHz, C_6D_6, 298 K): δ 8.14 (d, $^3J(^1H-^1H)$ = 8.4 Hz, 2H, *o-H*), 6.98 (d, $^3J(^1H-^1H)$ = 8.4 Hz, 2H, *m-H*), 2.38 (s, $J(^1H-^{117/119}Sn)$ = 18.3 Hz, 6H, NCH_2), 1.28 (s, 18H, $C(CH_3)_2$), 0.98 (s, 9 H, $C(CH_3)_3$). $^{13}C\{^1H\}$ NMR (100.63 MHz, C_6D_6, 298 K): δ 156.3 (s, COO), 131.3 (s, *aryl-C*), 129.3 (s, *aryl-C*), 128.5 (s, *aryl-C*), 125.4 (s, *aryl-C*), 69.6 (s, $J(^{13}C-^{117/119}Sn)$ = 25.7 Hz, NCH_2), 70.7 (s, $J(^{13}C-^{117/119}Sn)$ = 50.5 Hz, 29.9 Hz, $C(CH_3)_2O$), 34.8 (s, $C(CH_3)_3$), 31.4 (s, $J(^{13}C-^{117/119}Sn)$ = 35.8 Hz, $C(CH_3)_2$), 31.0 (s, $C(CH_3)_3$). $^{119}Sn\{^1H\}$ NMR (111.89 MHz, C_6D_6, 298 K): δ −416 (s, $\Delta\nu_{1/2}$ = 387 Hz). Anal. Calcd. for $C_{23}H_{37}NO_5Sn$ (%): C 52.5, H 7.1, N 2.7. Found: C 52.5, H 7.1, N 2.5. MS (ESI +): m/z = 216.3 $[C_{12}H_{26}NO_2]^+$, 234.3 $[N(CH_2CMe_2OH)_3 + H]^+$, 528.3 $[M + H]^+$, 583.4 $[M - OC(O)C_6H_4{}^tBu + N(CH_2CMe_2OH)_3]^+$.

*1-Chlorido-2,8,9-trioxa-5-aza-3,3,7,7,10,10-hexamethyl-stannatricyclo[3.3.3.0^{1,5}]undecane (**13**).* At room temperature, acetyl chloride (0.31 g, 3.95 mmol) was added dropwise to a stirred solution of **1** (1.68 g, 3.98 mmol) in dry toluene (100 mL). The mixture was heated at reflux for 1 h. The reaction mixture was slowly cooled to room temperature to afford colorless crystals. Recrystallization and subsequent washing with cold toluene (5 mL) gave **13** (1.10 g, 2.86 mmol, 72%) as colorless columns. ^{1}H NMR (300.13 MHz, $CDCl_3$, 298 K): δ 2.96 (s, $J(^1H-^{117/119}Sn)$ = 22.6 Hz, $^1J(^1H-^{13}C)$ = 138.8 Hz, 6H, NCH_2), 1.31 (s, $^1J(^1H-^{13}C)$ = 126.2 Hz, 18H, $C(CH_3)_2$). ^{1}H NMR (300.13 MHz, CD_2Cl_2, 215 K): δ 2.94 (s, $\Delta\nu_{1/2}$ = 39.3 Hz, 6H, NCH_2), 1.24 (s, $^1J(^1H-^{13}C)$ = 126.2 Hz, 18H, $C(CH_3)_2$).$^{13}C\{^1H\}$ NMR (75.48 MHz, $CDCl_3$, 298 K): δ 70.3 (s, $J(^{13}C-^{117/119}Sn)$ = 25.5 Hz, $C(CH_3)_2$), 70.2 (s, $J(^{13}C-^{117/119}Sn)$ = 52.8 Hz, NCH_2), 31.1 (s, $J(^{13}C-^{117/119}Sn)$ = 32.4 Hz, $C(CH_3)_2$). $^{13}C\{^1H\}$ NMR (75.48 MHz, CD_2Cl_2, 210 K): δ 70.1 (s, $J(^{13}C-^{117/119}Sn)$ = 23.6 Hz, $C(CH_3)_2$), 69.0 (s, $J(^{13}C-^{117/119}Sn)$ = 52.4 Hz, NCH_2), 30.5 (s, $J(^{13}C-^{117/119}Sn)$ = 32.4 Hz, $C(CH_3)_2$).$^{119}Sn\{^1H\}$ NMR (111.89 MHz, $CDCl_3$, 298 K): δ −243 (s). $^{119}Sn\{^1H\}$ NMR (111.89 MHz, CD_2Cl_2, 213 K): δ −235 (s) ^{119}Sn CP-MAS NMR (149.22 MHz): δ_{iso} −233, −236, −238, −239. Mp. 198 °C (decomposition). IR (nujol, ν/cm^{-1}) = 2922, 2853, 1461, 1377, 1287, 1190, 1160, 1068, 936, 920, 785, 657. Anal. Calcd. for $C_{12}H_{24}ClNO_3Sn$ (%): C 37.5, H 6.3, N 3.6. Found: C 37.4, H 6.2, N 3.5. MS (ESI +): m/z = 216.2 $[C_{12}H_{26}NO_2]^+$, 234.2 $[N(CH_2CMe_2OH)_3 + H]^+$, 350.0 $[M - Cl]^+$, 391.1 $[M - Cl + MeCN]^+$. Molecular weight (osmometric, $CHCl_3$): Calcd. for $C_{12}H_{24}ClNO_3Sn$: 385.1 g/mol. Found: 427.6 g/mol.

*1-Bromido-2,8,9-trioxa-5-aza-3,3,7,7,10,10-hexamethyl-stannatricyclo[3.3.3.0^{1,5}]undecane (**14**).* Trimethylbromidosilane (0.50 g, 3.27 mmol) was added dropwise to a stirred solution of **1** (1.37 g, 3.25 mmol) in dry toluene (150 mL) at room temperature. After it was stirred for 48 h at room temperature the mixture was concentrated to 80 mL under reduced pressure. The remaining suspension was heated to reflux, filtered and after slow cooling to room temperature compound **14** (1.21 g, 2.82 mmol, 87%) was obtained as colorless crystals. ^{1}H NMR (400.13 MHz, CD_2Cl_2, 298 K): δ 2.96 (s, $J(^1H-^{117/119}Sn)$ = 22.2 Hz, $^1J(^1H-^{13}C)$ = 138.9 Hz, 6H, NCH_2), 1.30 (s, $^1J(^1H-^{13}C)$ = 126.1 Hz, 18H, $C(CH_3)_2$). $^{13}C\{^1H\}$ NMR (100.63 MHz, CD_2Cl_2, 298 K): δ 70.9 (s, $J(^{13}C-^{117/119}Sn)$ = 28.7 Hz, $C(CH_3)_2$), 70.3 (s, $J(^{13}C-^{117/119}Sn)$ = 54.0 Hz, NCH_2), 31.2 (s, $J(^{13}C-^{117/119}Sn)$ = 32.1 Hz, $C(CH_3)_2$). $^{119}Sn\{^1H\}$ NMR (111.89 MHz, CD_2Cl_2, 298 K): δ −284 (s, $\Delta\nu_{1/2}$ = 15.72 Hz). ^{13}C CP-MAS NMR (100.63 MHz, 300 K, Supporting Information Figure S7): δ_{iso} 73.8 (s, $C(CH_3)_2O$, NCH_2)), 36.3, 35.4 (CCH_3). ^{119}Sn CP-MAS NMR (149 MHz, 300 K): δ_{iso} −260 (s), −271 (s), −282 (s), −290.1 (s). Mp. 180 °C (decomposition). Anal. Calcd. (%) for $C_{12}H_{24}BrNO_3Sn$: C 33.6, H 5.6, N 3.3. Found: C 33.7, H 5.8, N 3.1. MS (ESI +): m/z = 234.2 $[N(CH_2CMe_2OH)_3 + H]^+$, 430.1 $[M + H]^+$, 583.3 $[M - Br + N(CH_2CMe_2OH)_3]^+$.

*1-Iodido-2,8,9-trioxa-5-aza-3,3,7,7,10,10-hexamethyl-stannatricyclo[3.3.3.0^{1,5}]undecane (**15**).* The procedure is the same as described for compound **14**, with **1** (3.06 g, 7.25 mmol) and trimethyliodidosilane (1.45 g, 7.25 mmol) as starting materials. Recrystallization from toluene gave **15** (3.19 g, 6.70 mmol, 92%) as colorless columns. ^{1}H NMR (400.13 MHz, CD_2Cl_2, 298 K): δ 2.95 (s, $J(^1H-^{117/119}Sn)$ = 22.1 Hz, $^1J(^1H-^{13}C)$ = 138.7 Hz, 6H, NCH_2), 1.29 (s, $^1J(^1H-^{13}C)$ = 126.1 Hz, 18H, $C(CH_3)_2$). $^{13}C\{^1H\}$ NMR (100.63 MHz, CD_2Cl_2, 298 K): δ 71.3 (s, $J(^{13}C-^{117/119}Sn)$ = 33.1 Hz, $C(CH_3)_2$), 70.2 (s, $J(^{13}C-^{117/119}Sn)$ = 53.7 Hz, NCH_2), 31.2 (s, $J(^{13}C-^{117/119}Sn)$ = 30.5 Hz, $C(CH_3)_2$). $^{119}Sn\{^1H\}$ NMR (112 MHz, CD_2Cl_2, 298 K): δ −396 (s). mp: 232 °C. Anal. Calcd. for $C_{12}H_{24}INO_3Sn$ (%): C 30.3, H 5.1, N 2.9. Found: C 30.3, H 5.1, N 2.7. MS (ESI +): m/z = 216.2 $[C_{12}H_{26}NO_2]^+$, 234.2 $[N(CH_2CMe_2OH)_3 + H]^+$, 306.2 $[N(CH_2CMe_2OH)_3 + CH_2CMe_2OH]^+$, 349.9 $[M - I]^+$, 477.9 $[M + H]^+$.

*1,4-Bis[(2,8,9-trioxa-5-aza-3,3,7,7,10,10-hexamethyl-1-stannatricyclo[3.3.3.0^{1,5}]undecane-1-yloxy)dimethylsilyl]benzene (**16**).* The procedure is the same as described for compound **3**, with **1** (2.30 g, 5.45 mmol) and 1,4-bis(hydroxydimethylsilyl)benzene (0.62 g, 2.74 mmol) as starting materials. The concentrated toluene suspension was filtered and washed with cold toluene. Crystallization from dichloromethane/hexane gave **16** (1.96 g, 2.12 mmol, 78%) as colorless crystalline solid. ^{1}H NMR (300.13 MHz, CD_2Cl_2, 296 K): δ 7.63 (s, $J(^1H-^{13}C)$ = 146.0 Hz/148.8 Hz, 4H, *aryl-H*), 2.88 (s, $J(^1H-^{117/119}Sn)$ = 18.3 Hz, 12H, NCH_2), 1.26 (s, $^1J(^1H-^{13}C)$ = 125.8 Hz, 36H, $C(CH_3)_2$), 0.35 (s, $^1J(^1H-^{13}C)$ = 118.4 Hz, $^2J(^1H-^{29}Si)$ = 16.3 Hz, $^4J(^1H-^{119}Sn)$ = 6.3 Hz, 12H, $SiCH_3$). $^{13}C\{^1H\}$ NMR (100.63 MHz, CD_2Cl_2, 296 K): δ 142.5 (s, *i-C*), 132.5 (s, *aryl-C*), 70.6 (s, $J(^{13}C-^{117/119}Sn)$ = 50.2 Hz, NCH_2), 69.2 (s, $J(^{13}C-^{117/119}Sn)$ = 18.2 Hz, $C(CH_3)_2O$), 31.3 (s, $J(^{13}C-^{117/119}Sn)$ = 31.5 Hz, $C(CH_3)_2$), 1.73 (s, $^1J(^{13}C-^{29}Si)$ = 59.6 Hz, $^3J(^{13}C-^{119}Sn)$ = 7.2 Hz, $SiCH_3$). $^{29}Si\{^1H\}$ NMR (60 MHz, CD_2Cl_2, 296 K): δ 2.2 (s, $^1J(^{29}Si-^{13}C)$ = 59.6 Hz, $^2J(^{29}Si-^{117/119}Sn)$ = 26.4 Hz). $^{119}Sn\{^1H\}$ NMR (111.89 MHz, CD_2Cl_2, 296 K): δ −313 (s, $J(^{119}Sn-^{13}C)$ = 51 Hz, $^2J(^{119}Sn-^{29}Si)$ = 27 Hz). mp: 315−316 °C (decomposition). Anal. Calcd for $C_{34}H_{64}N_2O_8Si_2Sn_2$ (%): C 44.3, H 7.0, N 3.0. Found: C 43.3, H 6.8, N 2.9. MS (ESI+): m/z = 216.2 $[C_{12}H_{26}NO_2]^+$, 234.2 $[N(CH_2CMe_2OH)_3 + H]^+$, 583.4 $[N(CH_2CMe_2O)_3Sn + N(CH_2CMe_2OH)_3]^+$, 715.3 $[N(CH_2CMe_2O)_3SnOSn(OCMe_2CH_2)_3N + H]^+$, 773.5, 867.1,

dx.doi.org/10.1021/ic202179e | Inorg. Chem. 2012, 51, 1041−1056

932.2, 999.3, 1062.4 $[N(CH_2CMe_2O)_3SnOSn(OCMe_2CH_2)_3N + N(CH_2CMe_2O)_3Sn]^+$, 1156.8 $[M + N(CH_2CMe_2OH)_3 + H]^+$, 1221.3, 1325.4, 1444.3.

Crystallography. All intensity data were collected with an Xcalibur2 CCD diffractometer (Oxford Diffraction) using Mo−Kα radiation at 110 K. The structures were solved with direct methods using SHELXS-97[33] and refinements were carried out against F^2 by using SHELXL-97.[33] All non-hydrogen atoms were refined using anisotropic displacement parameters. The C−H hydrogen atoms were positioned with idealized geometry and refined using a riding model. In compound **5**·0.25 C_7H_8 and in compound **15**·C_7H_8 the solvate molecules were found severely disordered and removed by Squeeze-(Platon)[34] to improve the main part of the structure. CCDC-847238 (**3**), CCDC-847239 (**4**), CCDC-847240 (**5**·0.25 C_7H_8), CCDC-847241 (**6**), CCDC-847242 (**7**), CCDC-847243 (**8**), CCDC-847244 (**11**), CCDC-847245 (**12**), CCDC-847246 (**13**), CCDC-847247 (**14**), CCDC-847248 (**15**·C_7H_8), and CCDC-847249 (**16**) contain the supplementary crystallographic data for this paper. These data can be obtained free of charge from The Cambridge Crystallographic Data Centre via www.ccdc.cam.ac.uk/data_request/cif.

Electrochemistry. An EG&G 362 and a PAR-2273 potentiostats were used for voltammetry and chronoamperometric experiments. The 2 mm in diameter glassy carbon (GC) and a 0.5 mm Pt disk working electrodes were used. A 2.5 × 50 mm GC rod, separated from the analyte by a sintered glass diaphragm, was used as counter electrode. Peak potentials E_p were measured relative to Pt wire electrode electrochemically covered with polypyrrole and corrected using in situ reversible system ferrocenium/ferrocene ($E^\circ_{Fc+/Fc}$(DMSO) = 0.31 V vs SCE[35]). For EPR-coupled electrochemical experiments, a 1.8 mm cylindrical three-electrode version of the four-electrode cell[36] with Pt spiral working electrode was used. Cell polarization was starting from E = 0 V with the increments of 50 mV until the appearance of an EPR signal.

As supporting electrolytes, Bu_4NPF_6 or Bu_4NBF_4 (as 0.1 M solution) were used, activated in vacuum at 80 °C for 10 h prior to use.

For conductivity measurements, a conductimeter Jenway 4320 was used. Multispec 1500 (Schimadzu) UV−vis spectrometer and X-band Bruker EMX EPR spectrometer (9.46 GHz) coupled to a standard rectangular cavity were used for spectro-electrochemical experiments. EPR spectra were simulated using Bruker WINEPR SimFonia software.[37]

DFT Calculations. Geometry optimization, frequency and NBO analyses were performed at DFT B3LYP/DGDZVP//HF/6-311G level using GAUSSIAN 03 package.[38]

RESULTS AND DISCUSSION

The reaction of tin tetra-*t*-butoxide, Sn(O-*t*-Bu)$_4$, and tin tetra-*i*-propoxide, Sn(O-*i*-Pr)$_4$, with tris(2-hydroxy-2-methyl-propyl)-amine, $N(CH_2CMe_2OH)_3$, gave the novel 1-alkoxy-stannatranes **1** and **2**, respectively (Scheme 4).

Scheme 4. Syntheses of 1-alkoxy-stannatranes.

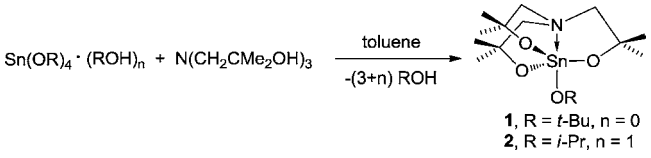

1, R = *t*-Bu, n = 0
2, R = *i*-Pr, n = 1

Both compounds are highly sensitive to moisture, well soluble in dichloromethane, tetrahydrofurane, and diethylether and show moderate solubility in toluene and benzene. Especially compound **1** proved to be a rather useful starting material for the synthesis of a variety of inorganic stannatranes. Thus, in an acid−base type reaction the treatment of the *t*-butoxystannatrane **1** with phenol, thiophenol and aminoethanol derivatives, diphenyldithiophosphinic acid, $Ph_2P(S)SH$, and *p*-*t*-butyl benzoic acid, *p*-*t*-BuC_6H_4COOH, gave the stannatranes **3**−**12**, respectively, in high yields (Scheme 5).

The synthesis of the halogenido-substituted stannatranes **13**−**15** was achieved by the reaction of compound **1** with acetyl chloride, $CH_3C(O)Cl$, and trimethylhalogenido silanes, Me_3SiX (X = Br, I), respectively (Scheme 5).

The spacer-bridged dinuclear stannatrane **16** containing a Sn−O−Si bond sequence was obtained by the reaction of compound **1** with 1,4-bis(hydroxydimethylsilyl)benzene $C_6H_4(SiMe_2OH)_2$-1,4 (Scheme 6).

The stannatranes **3**−**8** and **11**−**16** are colorless or yellowish (**5**·0.25C_7H_8) crystalline materials. Notably, on exposure to air and light the color of the iodido-substituted stannatrane **15**·C_7H_8 changed to yellow. Compound **9** was obtained as yellow amorphous solid and compound **10** as yellowish oil that solidified upon standing. All compounds are soluble in benzene, toluene, dichloromethane and tetrahydrofurane, but at room temperature the chlorido and bromido derivatives **13** and **14** are only well soluble in dichloromethane or chloroform.

The molecular structures of **3**, **4**, **5**·0.25C_7H_8, **6**−**8**, **11**−**14**, **15**·C_7H_8, and **16**, as determined by single-crystal X-ray diffraction analysis, are shown in Figures 1−12. Selected bond distances and bond angles are summarized in Tables 1−3. The unit cells of compounds **3**, **5**·0.25C_7H_8, **11**, and **12** each contain two crystallographic independent molecules *a* and *b* the geometric parameters of which differ only slightly. Consequently, only the molecules **3a**, **5a**, **11a**, and **12a** are shown whereas **3b**, **5b**, **11b**, and **12b** are given in the Supporting Information (Figures S1−S4).

Similar to parent titanatranes $N(CH_2CMe_2O)_3TiOR$ (R = *i*-Pr; 2,6-di-*i*−Pr−C_6H_3)[30,39] or 1-*tert*-butyl-stannatrane $N(CH_2CH_2O)_3$-Sn-*t*-Bu[16] and in contrast to the related oxygen bridged tin(II) alkoxide $[HOCMe_2CH_2N(CH_2CMe_2O)_2Sn]_2$[26] or the oxygen bridged 1-methyl-stannatrane $[N(CH_2CH_2O)_3SnMe]_3{\cdot}6H_2O$,[15] the stannatranes **3**−**8** and **11**−**16** adopt each a monomeric structure in the solid state, mainly due to the steric protection by the methyl groups of the atrane framework. As result of the intramolecular N→Sn coordination the tin atoms, except for the benzoate-substituted compound **12**, show each a distorted trigonal bipyramidal configuration with the N(1)/N(2) and the O(4)/O(104) respectively S(1)/S(2) atoms occupying the axial positions. The equatorial positions are occupied by the O(1)−O(3) and O(101)−O(103) atoms, respectively. The tin atom is displaced from the plane $E(O_{equatorial})$ defined by the oxygen atoms O(1)−O(3) or O(101)−O(103) in direction to the exocyclic ligand (Table 4). The geometrical goodness $\Delta\Sigma(\vartheta)^\circ$[40] of the trigonal bipyramidal configuration of the tin atoms in compounds **3**−**8**, **11**, and **13**−**16** falls in the range between 55.4° (**8**) and 64.6° (**5**) and indicates strong distortion from the ideal geometry (Table 4). The N−Sn distances vary between 2.295(3) Å (**12**) and 2.232(2) Å (**5b**) with the latter being one of the two shortest Sn−N distance reported for stannatranes. The shortest such bond so far (2.231(7) Å) was reported for $N[CH_2C(O)O]_3Sn(CH_2)_3N(O)Me_2$.[17] The N−Sn distances in the 1-halogenido-substituted stannatranes **13**−**15**·C_7H_8 decreases in the order X = Cl → I (**13**, X = Cl, *d*(N−Sn) = 2.268 (12) Å; **14**, X = Br, *d*(N−Sn) = 2.263(7) Å; **15**·C_7H_8, X = I, *d*(N−Sn) = 2.279(6) Å). Remarkably, for 1−halogenido-carbastannatranes $N(CH_2CH_2CH_2)_3SnX$ (X = Cl, *d*(N−Sn) = 2.37(3)/2.384(4) Å; X = Br, *d*(N−Sn) = 2.28(2) Å; X = I, *d*(N−Sn) = 2.375(6) Å) the strongest donor interaction was found for X = Br which was explained by counteractive effects of electronegativity and lone pair interaction

dx.doi.org/10.1021/ic202179e | Inorg. Chem. 2012, 51, 1041−1056

Scheme 5. Synthesis of the novel stannatranes 3−15.

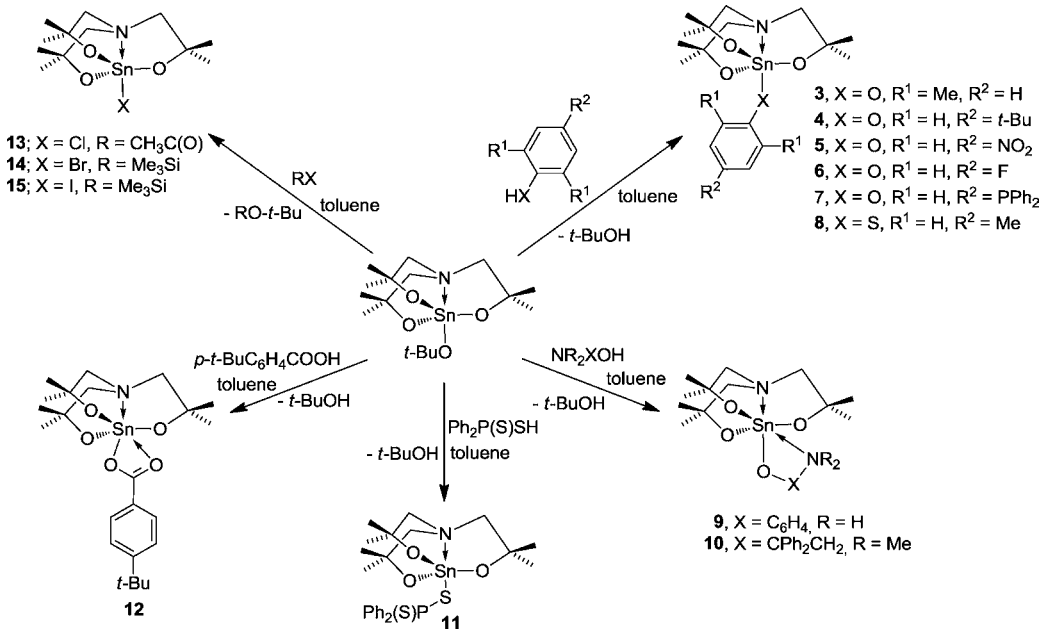

Scheme 6. Synthesis of compound 16.

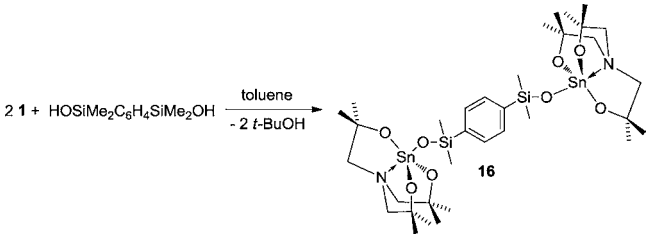

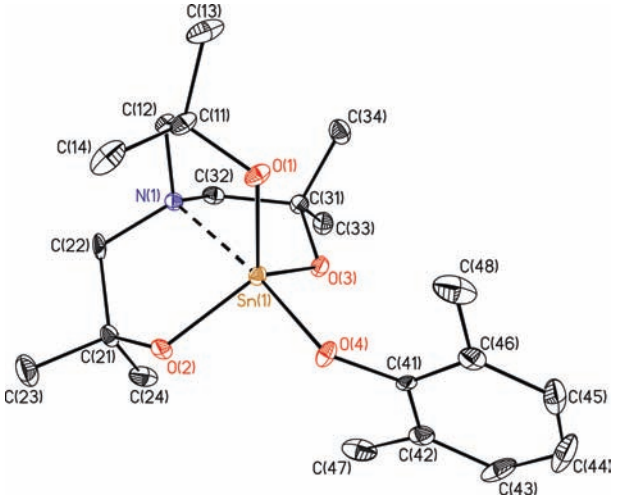

Figure 1. Molecular structure of compound **3** (molecule **3a**, ORTEP presentation at 30% probability of the depicted atoms and atom numbering scheme.

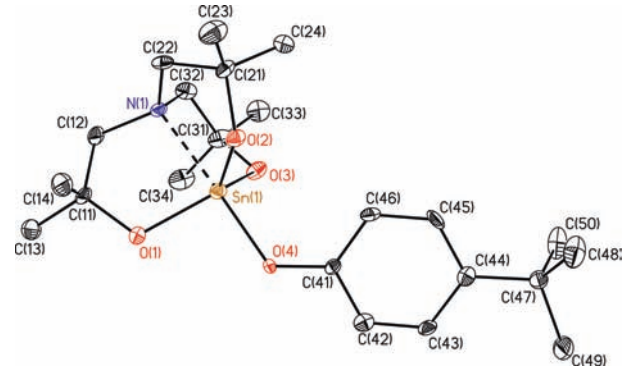

Figure 2. Molecular structure of compound **4** (ORTEP presentation at 30% probability of the depicted atoms and atom numbering scheme).

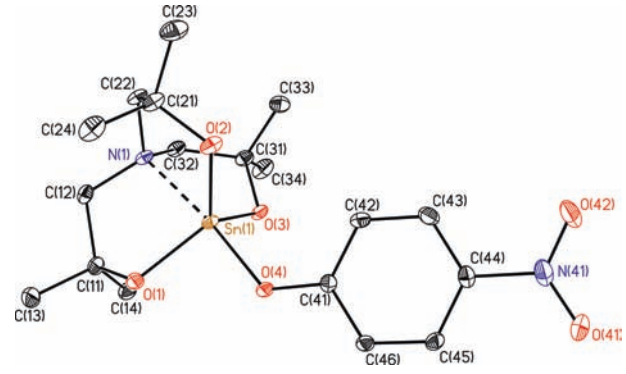

Figure 3. Molecular structure of compound **5**·0.25C_7H_8 (molecule **5a**, ORTEP presentation at 30% probability of the depicted atoms and atom numbering scheme). The solvent molecule was removed by Platon Squeeze.[34]

of the halogen substituents.[40] As typical for stannatrane-type compounds, the five membered rings of the atrane framework adopt uniform envelope conformations and make the molecules chiral. The combinations of stereoisomers and crystallographically independent molecules in the unit cell are summarized in Table 5. Looking along the X−Sn−N axis, the unit cells of the stannatranes **3**, **5**·0.25C_7H_8, and **11** each contain two crystallographically independent molecules *a* and *b* that exist as pairs of enantiomers ($\mathbf{3a}_\Delta$, $\mathbf{3b}_\Delta/\mathbf{3a}_\Lambda$, $\mathbf{3b}_\Lambda$). The unit cells of the stannatranes **4**, **14**, and **15**·C_7H_8 each contain only one crystallographically independent molecule as single enantiomers

dx.doi.org/10.1021/ic202179e | *Inorg. Chem.* 2012, 51, 1041−1056

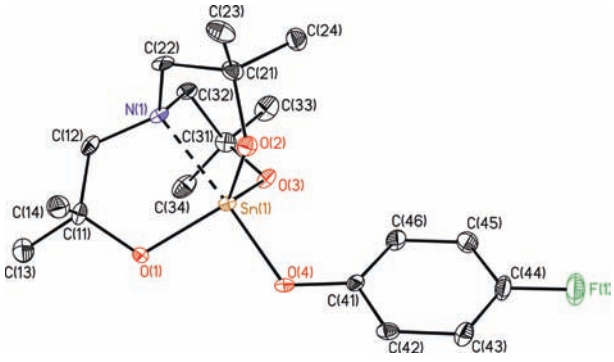

Figure 4. Molecular structure of compound **6** (ORTEP presentation at 30% probability of the depicted atoms and atom numbering scheme).

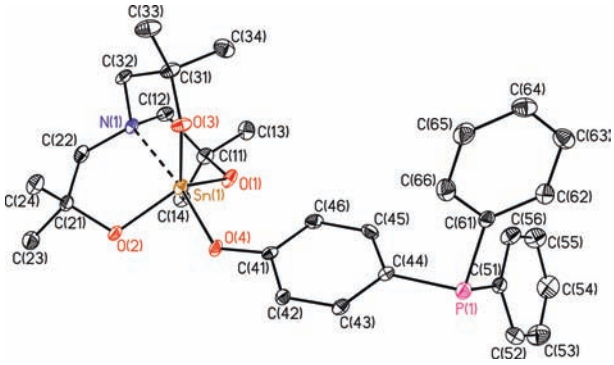

Figure 5. Molecular structure of compound **7** (ORTEP presentation at 30% probability of the depicted atoms and atom numbering scheme).

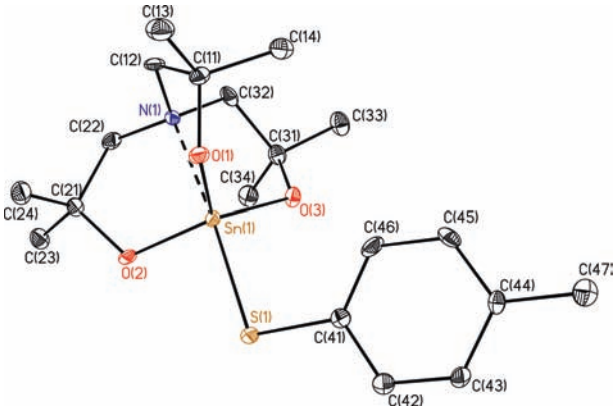

Figure 6. Molecular structure of compound **8** (ORTEP presentation at 30% probability of the depicted atoms and atom numbering scheme).

with clockwise ($\mathbf{4}_{\Delta}$) and anticlockwise ($\mathbf{14}_{\Lambda}$, $\mathbf{15}_{\Lambda}$) orientation of the propellers whereas the unit cells of compounds **6**–**8** each contain one crystallographically independent molecule as well, but as pair of enantiomers $\mathbf{6}_{\Delta}/\mathbf{6}_{\Lambda}$, $\mathbf{7}_{\Delta}/\mathbf{7}_{\Lambda}$, and $\mathbf{8}_{\Delta}/\mathbf{8}_{\Lambda}$. The unit cell of the benzoate-substituted stannatrane **12** contains two crystallographically independent molecules $\mathbf{12a}_{\Delta}$ and $\mathbf{12b}_{\Lambda}$, both as single enantiomers. The unit cell of the spacer-bridged distannatrane **16** contains a single diastereomer in which one stannatrane moiety shows clockwise and the other one shows anticlockwise orientation. A special situation is observed for the chlorido-substituted stannatrane **13**. The unit cell contains

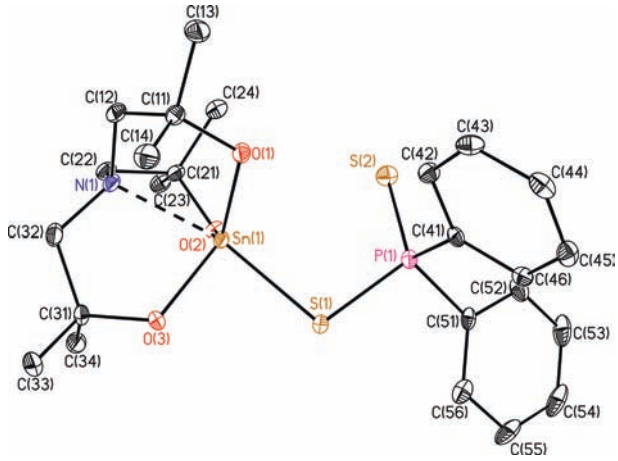

Figure 7. Molecular structure of compound **11** (molecule **11a**, ORTEP presentation at 30% probability of the depicted atoms and atom numbering scheme).

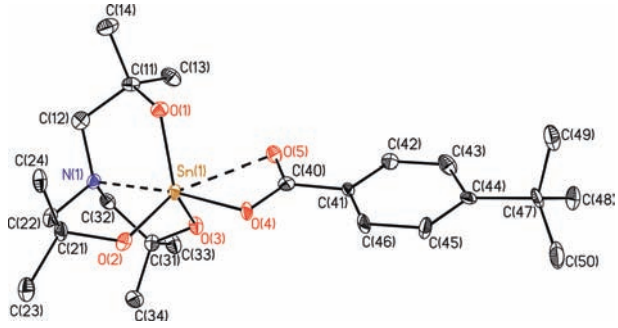

Figure 8. Molecular structure of compound **12** (molecule **12a**, ORTEP presentation at 30% probability of the depicted atoms and atom numbering scheme).

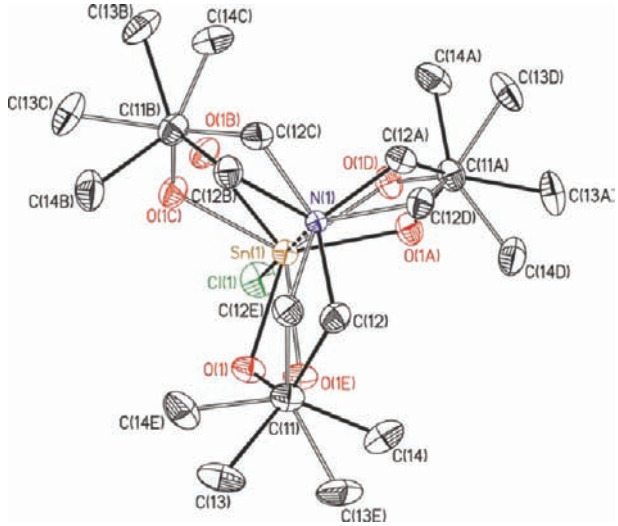

Figure 9. Molecular structure of compound **13** (ORTEP presentation at 30% probability of the depicted atoms and atom numbering scheme). Only one-half of one atrane propeller is present in the asymmetric unit. The other half and the two other propellers are created by symmetry operations (symm. codes (A) $-x + 1, x - y + 1, z$; (B) $-x + y, -x + 1, z$; (C) $-y + 1, -x + 1, z$; (D) $-x + y, y, z$; (E) $x, x - y + 1, z$).

a single crystallographically independent molecule the atrane cage of which is, however, completely disordered in such a

dx.doi.org/10.1021/ic202179e | *Inorg. Chem.* 2012, 51, 1041–1056

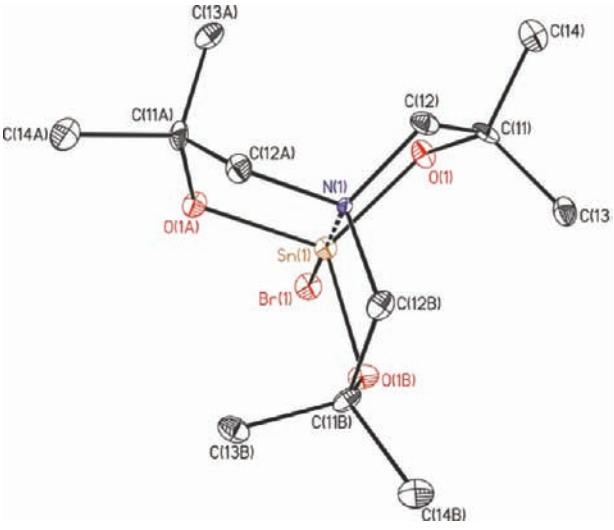

Figure 10. Molecular structure of compound **14** (ORTEP presentation at 30% probability of the depicted atoms and atom numbering scheme). Symmetry codes (A) $-x + y, -x + 1, z$; (B) $-y + 1, x - y + 1, z$.

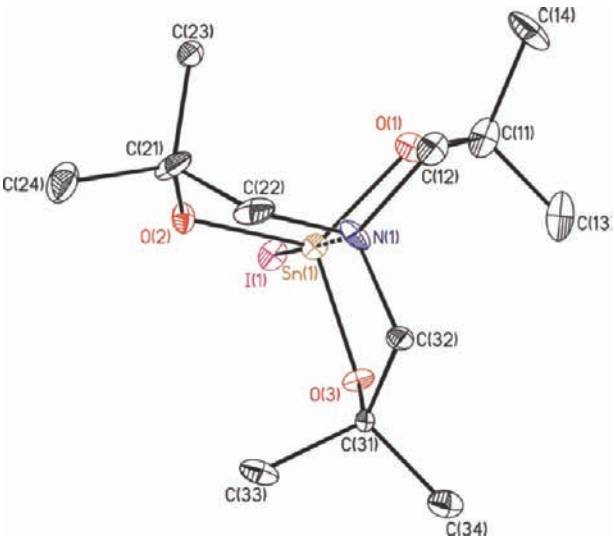

Figure 11. Molecular structure of compound **15**·C_7H_8 (ORTEP presentation at 30% probability of the depicted atoms and atom numbering scheme). The solvent molecule was removed by Platon Squeeze.[34]

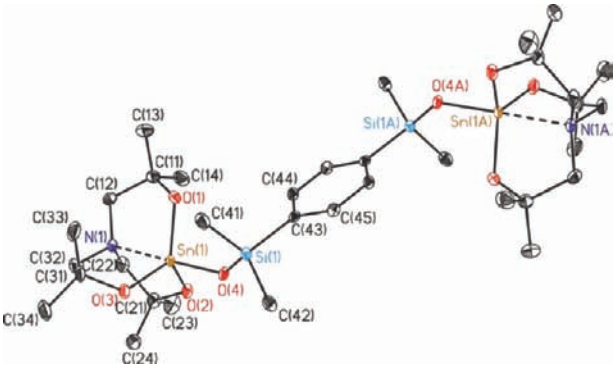

Figure 12. Molecular structure of compound **16** (ORTEP presentation at 30% probability of the depicted atoms and atom numbering scheme). Symmetry code (A) $-x + 1, -y + 1, -z + 1$.

way that the structure can be interpreted in terms of a superposition of four pairs of enantiomers of different conformations (Figure 13).

The same result was obtained from the analysis of X-ray diffraction data recorded at room temperature. The interpretation is supported by the ^{119}Sn CP MAS spectrum (Supporting Information, Figure S5) showing four equally intense resonances at δ_{iso} −233, −236, −238, and −239. The X-ray powder diffraction measurement confirms the homogeneity of the bulk material (Supporting Information, Figure S6). Strange enough, four equally intense ^{119}Sn resonances are also observed for the bromido-substituted stannatrane **14** (δ_{iso} −260, −270, −282, −290) (Supporting Information, Figure S7, ^{13}C CP MAS Figure S8) the molecular structure of which (obtained from X-ray diffraction data measured at low temperature) shows a single enantiomer only (see above). The X-ray measurement of the cell parameters of seven single crystals revealed the same parameters. Consequently, it is rather unlikely that the bulk material used for the ^{119}Sn CP MAS spectrum is a mixture composed of single crystals containing different conformers. This is supported by a X-ray powder diffraction measurement confirming this conclusion as the data obtained fit reasonably well with the simulated data obtained from the single crystal measurement (Supporting Information, Figure S9). Given the fact that during the ^{119}Sn CP MAS data acquisition the sample heats up to approximately 60 °C it might be that at this temperature all four pairs of conformers are formed.

Compared to the stannatranes **3**−**8**, **11**, and **13**−**16** the tin atom of the benzoate-substituted stannatrane **12** exhibits an even more distorted trigonal bipyramidal configuration as result of the unisobidentate coordination mode of the benzoate substituent associated with intramolecular O(5) → Sn(1)/O(105) → Sn(2) interactions at distances of 2.574(3) (**12a**) and 2.473(3) Å (**12b**) that are considerably shorter than the sum of the van der Waals radii (3.70 Å) of the corresponding atoms. These interactions are also reflected in a widening of the O(1)−Sn(1)−O(3)/O(101)−Sn(2)−O(103) angles to 130.0(1) (**12a**) and 125.0(1)° (**12b**). Moreover, a short O→Sn interaction causes a long N→Sn interaction and vice versa.

The ^{119}Sn solution NMR spectra of the 1-alkoxido- and aryloxido-substituted stannatranes **1**−**7**, and **16**, respectively, show single resonances between δ −311 (**7**) and δ −333 (**3**). Surprisingly, these signals are high- and not, as expected, low-frequency shifted with respect to tetracoordinated Sn(O-*t*-Bu)$_4$ (δ −374[41,42]). For the latter compound low-frequency shifts at δ −510 and δ −420 have been reported upon addition of *t*-butanol and pyridine, respectively.[41] For a reliable interpretation of the chemical shifts of compounds **1**−**7** and **16** with respect to the strength of intramolecular N→Sn coordination, a model compound such as HC(CH$_2$CMe$_2$O)$_3$SnOR (R = alkyl, aryl) that lacks such an interaction would be needed which is, however not easy to be synthesized. The thiophenolato- and diphenylphosphinodithiolato- substituted stannatranes **8** and **11** show single ^{119}Sn NMR resonances at δ −227 (**8**) and δ −246 (**11**), respectively. The high-frequency shift of the two latter compounds with respect to the compounds mentioned above is the result of the introduction of sulfur atoms at the 1-position. The only slightly high field shift of the resonance observed for **11** compared to the thiophenolato-substituted derivative **8** indicates pentacoordination of the tin atom in **11** without additional P═S → Sn coordination as already shown for the solid state. The halogenido-substituted stannatranes **13**−**15** show single resonances at δ −243 (δ −235 at 213 K, **13**), δ −248 (**14**), and δ

dx.doi.org/10.1021/ic202179e | Inorg. Chem. 2012, 51, 1041−1056

Table 1. Selected Bond Distances (Å) and Angles (deg) for Compounds 3−8

	3 (X = O(4))	**4** (X = O(4))	**5**·0.25C_7H_8 (X = O(4))	**6** (X = O(4))	**7** (X = O(4))	**8** (X = S(1))
Sn(1)−O(1)	1.965(2)	1.972(3)	1.963(2)	1.971(4)	1.980(2)	1.987(2)
Sn(1)−O(2)	1.982(2)	1.974(2)	1.970(2)	1.969(4)	1.965(2)	1.973(2)
Sn(1)−O(3)	1.971(2)	1.970(3)	1.975(2)	1.981(4)	1.969(2)	1.984(2)
Sn(1)−X	1.960(2)	1.975(2)	1.994(2)	1.976(4)	1.989(2)	2.411(1)
Sn(1)−N(1)	2.255(2)	2.258(3)	2.248(2)	2.254(5)	2.250(3)	2.284(3)
Sn(2)−O(101)	1.975(2)		1.972(2)			
Sn(2)−O(102)	1.980(2)		1.963(2)			
Sn(2)−O(103)	1.975(2)		1.964(2)			
Sn(2)−O(104)	1.970(2)		1.987(2)			
Sn(2)−N(2)	2.253(3)		2.232(2)			
O(1)−Sn(1)−O(2)	117.1(1)	115.0(1)	119.7(1)	118.2(2)	117.1(1)	117.6(1)
O(1)−Sn(1)−O(3)	115.8(1)	120.1(1)	118.1(1)	116.1(2)	116.5(1)	117.7(1)
O(1)−Sn(1)−X	100.4(1)	95.7(1)	91.2(1)	94.9(2)	104.3(1)	99.4(1)
O(1)−Sn(1)−N(1)	82.3(1)	82.7(1)	82.8(1)	82.5(2)	82.7(1)	80.4(1)
O(2)−Sn(1)−O(3)	121.5(1)	120.0(1)	117.0(1)	120.4(2)	121.4(1)	117.4(1)
O(2)−Sn(1)−X	91.9(7)	99.4(1)	101.1(1)	96.5(2)	90.5(1)	95.3(1)
O(2)−Sn(1)−N(1)	81.7(1)	82.3(1)	82.0(1)	82.2(2)	82.5(1)	81.5(1)
O(3)−Sn(1)−X	101.6(1)	97.3(1)	100.7(1)	101.6(2)	98.0(1)	102.6(1)
O(3)−Sn(1)−N(1)	82.3(1)	82.6(1)	82.3(1)	82.3(2)	82.3(1)	80.9(1)
N(1)−Sn(1)−X	173.6(1)	178.1(1)	174.0(1)	176.0(2)	171.8(1)	176.1(1)
Sn(1)−X−C(41)	133.9(2)	124.8(3)	128.2(1)	124.1(3)	130.0(2)	105.2(1)
O(101)−Sn(2)−O(102)	117.2(1)		115.0(1)			
O(101)−Sn(2)−O(103)	119.9(1)		118.8(1)			
O(101)−Sn(2)−O(104)	102.8(1)		103.5(1)			
O(101)−Sn(2)−N(2)	82.6(1)		83.3(1)			
O(102)−Sn(2)−O(103)	117.7(1)		121.9(1)			
O(102)−Sn(2)−O(104)	98.3(1)		92.9(1)			
O(102)−Sn(2)−N(2)	82.4(1)		82.9(1)			
O(103)−Sn(2)−O(104)	91.9(1)		94.7(1)			
O(103)−Sn(2)−N(2)	82.1(1)		83.0(1)			
N(2)−Sn(1)−X	173.5(1)		173.1(1)			
Sn(2)−O(104)−C(141)	133.4(2)		133.0(2)			

Table 2. Selected Bond Distances (Å) and Angles (deg) for compounds 11 and 12

	11 (X = S, Y = P, *a*, *c* = 1, *b* = 3, *d* = 2)	**12** (X = O, Y = C, *a* = 4, *b* = 104, *c* = 40, *d* = 140)		**11** (X = S, Y = P, *a*, *c* =1, *b* = 3, *d* = 2)	**12** (X = O, Y = C, *a* = 4, *b* = 104, *c* = 40, *d* = 140)
Sn(1)−O(1)	1.979(2)	1.981(3)	Sn(2)−O(101)	1.984(2)	1.989(2)
Sn(1)−O(2)	1.977(2)	1.975(3)	Sn(2)−O(102)	1.975(2)	1.998(3)
Sn(1)−O(3)	1.983(2)	1.971(2)	Sn(2)−O(103)	1.974(2)	1.972(2)
Sn(1)−O(5)		2.574(3)	Sn(2)−O(105)		2.473(3)
Sn(1)−X(a)	2.428(1)	2.049(2)	Sn(2)−X(b)	2.429(1)	2.077(3)
Sn(1)−N(1)	2.288(2)	2.270(3)	Sn(2)−N(2)	2.276(2)	2.295(3)
O(1)−Sn(1)−O(2)	122.2(1)	108.1(1)	O(101)−Sn(2)−O(102)	114.5(1)	112.3(1)
O(1)−Sn(1)−O(3)	118.2(1)	130.0(1)	O(101)−Sn(2)−O(103)	119.7(1)	125.0(1)
O(1)−Sn(1)−O(5)		82.5(1)	O(101)−Sn(2)−O(105)		84.8(1)
O(1)−Sn(1)−X(a)	104.0(1)	102.7(1)	O(101)−Sn(2)−X(b)	87.8(1)	105.4(1)
O(1)−Sn(1)−N(1)	80.8(1)	81.2(1)	O(101)−Sn(2)−N(2)	81.0(1)	80.0(1)
O(2)−Sn(1)−O(3)	111.8(1)	115.1(1)	O(102)−Sn(2)−O(103)	118.7(1)	114.4(1)
O(2)−Sn(1)−O(5)		146.1(1)	O(102)−Sn(2)−O(105)		142.1(1)
O(2)−Sn(1)−X(a)	107.8(1)	90.5(1)	O(102)−Sn(2)−X(b)	106.0(1)	85.6(1)
O(2)−Sn(1)−N(1)	80.7(1)	81.9(1)	O(102)−Sn(2)−N(2)	81.3(1)	80.3(1)
O(3)−Sn(1)−O(5)		75.6(1)	O(103)−Sn(2)−O(105)		75.9(1)
O(3)−Sn(1)−X(a)	84.6(1)	100.8(1)	O(103)−Sn(2)−X(b)	102.8(1)	105.6(1)
O(3)−Sn(1)−N(1)	80.5(1)	81.2(1)	O(103)−Sn(2)−N(2)	80.8(1)	80.7(1)
O(4)−Sn(1)−O(5)		55.7(1)	O(104)−Sn(2)−O(105)		56.7(1)
N(1)−Sn(1)−X(a)	164.8(1)	172.2(1)	N(2)−Sn(2)−X(b)	168.4(1)	164.0(1)
N(1)−Sn(1)−O(5)		131.9(1)	N(2)−Sn(2)−O(105)		137.3(1)
Sn(1)−X(a)−Y(c)	102.3(1)	102.6(3)	Sn(2)−X(b)−Y(d)	103.9(1)	99.7(3)

dx.doi.org/10.1021/ic202179e | *Inorg. Chem.* 2012, 51, 1041−1056

Table 3. Selected Bond Distances (Å) and Angles (deg) for Compounds 13−16

	13 (X = Cl(1), *a* = 1*a*)	14 (X = Br(1), *a* = 1*a*))	15·C_7H_8 (X = I(1), *a* = 2)	16 (X = O(4), *a* = 2)
Sn(1)−O(1)	1.974(3)	1.973(3)	1.974(5)	1.968(2)
Sn(1)−O(2)			1.969(5)	1.970(2)
Sn(1)−O(3)			1.955(5)	1.972(2)
Sn(1)−X	2.338(5)	2.473(1)	2.676(1)	1.942(1)
Sn(1)−N(1)	2.268(12)	2.263(7)	2.279(6)	2.258(2)
O(1)−Sn(1)−O(a)	118.20(5)	118.05(4)	120.7(3)	118.4(1)
O(1)−Sn(1)−O(3)			117.9(2)	119.5(1)
O(1)−Sn(1)−X	97.77(10)	98.10(8)	98.6(2)	97.8(1)
O(1)−Sn(1)−N(1)	82.23(10)	81.90(8)	81.2(2)	81.3(1)
O(2)−Sn(1)−O(3)			115.5(2)	116.1(1)
O(2)−Sn(1)−X			97.1(2)	96.6(1)
O(2)−Sn(1)−N(1)			81.8(2)	82.3(1)
O(3)−Sn(1)−X			98.5(2)	100.2(1)
O(3)−Sn(1)−N(1)			82.7(2)	81.9(1)
N(1)−Sn(1)−X	180.000(3)	180.000(2)	178.6(2)	177.8(1)
Sn(1)−O(4)−Si(1)				133.2(1)

Table 4. Geometrical Goodness of the Trigonal Bipyramide $\Delta\Sigma(\vartheta)°$ and Distances $\Delta(E(O_{eq})-Sn)$ for Compounds 3−8 and 11−16 of Type $N(CH_2CMe_2O)_3SnX$

compound	X	$\Delta\Sigma(\vartheta)°/°$	$\Delta(E(O_{eq})-Sn)$ /Å
3	O-(1,2-Me_2)-C_6H_3	60.5(Sn1)/ 61.8(Sn2)	0.2720(2)/ 0.2636(2)
4	OC_6H_4-*p*-^{t}Bu	62.57	0.2565(3)
5·0.25C_7H_8	OC_6H_4-*p*-NO_2	61.8(Sn1)/ 64.6(Sn2)	0.2383(2)/ 0.2621(2)
6	OC_6H_4-*p*-F	61.8	0.2634(4)
7	OC_6H_4-*p*-PPh_2	62.2	0.2572(2)
8	SC_6H_4-*p*-Me	55.4	0.3134(3)
11	$SP(S)Ph_2$	55.8(Sn1)/ 56.3(Sn2)	0.3213(2)/ 0.3090(2)
12	$OC(O)C_6H_4$-*p*-^{t}Bu		0.2952(3)/ 0.3328(3)
13	Cl	61.3	0.2673(17)
14	Br	59.9	0.2779(8)
15·C_7H_8	I	58.0	0.2902(6)
16	$OSiMe_2C_6H_4SiMe_2O$−$Sn(OCMe_2CH_2)_3N$	59.4	0.2811(1)

Table 5. Stereoisomers of Independent Molecules m^x (*x* = *a*, *b*) with Right- (Δ) and Left-Handed (Λ) Propeller in the Unit Cell

compd.	stereoisomers in the unit cell
3, 5·0.25C_7H_8, 11	m^a_Δ, m^a_Λ, m^b_Δ, m^b_Λ
4	m^a_Δ
6−8	m^a_Δ, m^a_Λ
12	m^a_Δ, m^b_Λ
13	disordered atrane framework
14, 15·C_7H_8	m^a_Λ
16	$m^a_{\Delta,\Lambda}$

−396 (**15**) with the two former shifts being close to the values observed in their ^{119}Sn CP MAS spectra and indicating the structures in solution to be rather similar to those found in the solid state. The dramatic difference between the chemical shifts of the chlorido- and bromido-substituted stannatranes **13** and **14** on the one hand and the iodido-substituted stannatrane **15** on the other hand is traced to the much higher shielding effect of iodine and follows the trend observed for the chemical shifts in CS_2 of $SnCl_4$ (δ −150), $SnBr_4$ (δ −638), and SnI_4 (δ −1701).[43]

The ^{119}Sn and ^{13}C NMR spectra in CD_2Cl_2 at 213 and 210 K, respectively, of the chlorido-substituted stannatrane **13** show the interconversion of conformational isomers (Figure 13) to be fast on the corresponding NMR time scales. The ^{1}H NMR spectrum in CD_2Cl_2 at 213 K shows a broadening of the NCH_2 resonance ($\Delta\nu_{1/2}$ = 39.3 Hz).

Compared to the 1-alkoxido- and aryloxido-substituted stannatranes **1**−**7**, the *o*-aminophenolato- and the aminoethanolato-substituted stannatranes **9** (δ −432) and **10** (δ −462) show considerable low-frequency shifts indicating additional intramolecular N→Sn coordination in these compounds. A single broad resonance (δ (^{119}Sn) = −416 (s, $\Delta\nu_{1/2}$ = 387 Hz)) in the ^{119}Sn NMR spectrum of **12** (C_6D_6) hints at a fast equilibrium between penta- and hexacoordinated tin compounds that is shifted to the latter one.

Additional information about the identity of the stannatranes in solution is provided by ^{1}H and ^{13}C NMR spectroscopy including ^{1}H−^{13}C hsqc or ^{13}C-dept measurements. As expected, a high-frequency shift of the NCH_2 and CCH_3 resonances compared to the free trialkanolamine $N(CH_2CMe_2OH)_3$ is observed. The ^{1}H NMR spectra of compounds **1**−**16** show each one single resonance for the diastereotopic NCH_2 protons of the atrane framework with $J(^1H\text{-}^{117/119}Sn)$ coupling in the range of 16.1 Hz (**10**) to 23.5 Hz (**6**) (Table 6) and also one single resonance for the diastereotopic CCH_3 protons. Thus, compounds **1**−**16** possess pseudo−C_{3v} symmetry on the NMR time scale. The ^{1}H NMR spectra of the hexacoordinated tin compounds **9**, **10** and **12** (C_6D_6) show slightly lower $J(^1H\text{-}^{117/119}Sn)$ couplings of the atrane NCH_2 protons compared to the pentacoordinated 1-alkoxido- and aryloxido-substituted stannatranes **1** and **3**−**7** (Table 6). For compound **10**, the coordination of the dimethylamino group is verified by the $J(^1H\text{-}^{117/119}Sn)$ coupling of 12.2 Hz. In analogy, the ^{13}C NMR spectra show one single resonance for each of the chemically equivalent NCH_2, $C(CH_3)_2$ and $C(CH_3)_2$ carbon atoms. The signals for the NCH_2 and $C(CH_3)_2$ carbon atoms show $J(^{13}C\text{-}^{117/119}Sn)$ couplings in the range of 46.6 Hz (**2**) to 54.0 Hz (**14**) and 17.5 Hz (**2**) to 33.1 Hz (**15**), respectively (Table 6).

The ESI-MS data indicate high reactivity of the Sn−X bond as well as a notable stability of the atrane framework. Thus, for compounds **1**−**16** either the mass cluster of the atrane framework (m/z = 350.1 $[N(CH_2CMe_2O)_3Sn]^+$) or mass clusters of aggregates containing the atrane framework are present in the

dx.doi.org/10.1021/ic202179e | *Inorg. Chem.* 2012, 51, 1041−1056

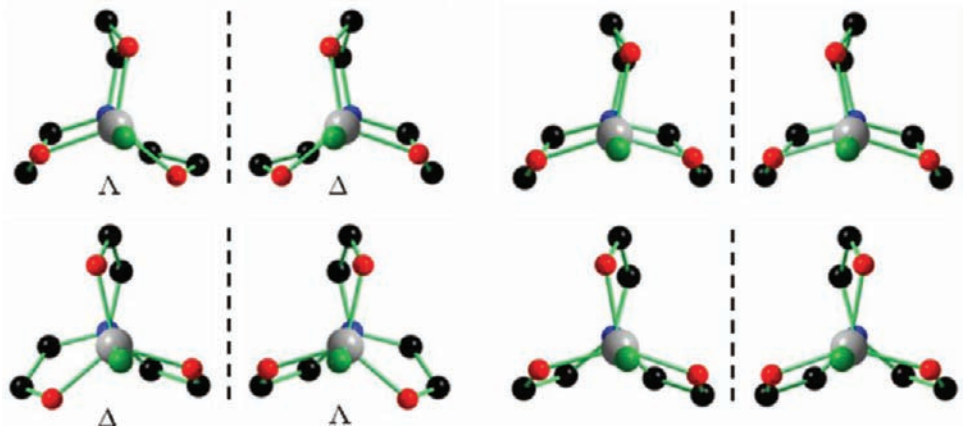

Figure 13. Four pairs of enantiomers of compound **13** by different conformations of the atrane propellers.

Table 6. Selected NMR Data of $N(CH_2CMe_2O)_3SnX$

compd.	X	δ ^{119}Sn	$J(^1H_2C-^{117/119}Sn)$ /Hz	$J(^{13}CH_2-^{117/119}Sn)$ /Hz	$J(^{13}CMe_2-^{117/119}Sn)$ /Hz	$J(^{13}CH_3-^{117/119}Sn)$ /Hz
1	*t*-BuO	−319	20.9	48.4	21.6	30.4
2	*i*-PrO	−312		46.6	17.5	30.4
3	2,6-$Me_2C_6H_3O$	−333	21.3	49.4	21.1	32.1
4	*p*-*t*-BuC_6H_4O	−322	23.3	49.5	19.1	31.2
5	*p*-$NO_2C_6H_4O$	−315	23.3	50.6	18.9	31.8
6	*p*-FC_6H_4O	−313	23.5	49.4	18.7	31.1
7	*p*-$PPh_2C_6H_4O$	−311	23.4	50.0	19.1	27.5
8	*p*-MeC_6H_4S	−227	21.0	48.0	30.6	27.5
9	*o*-$NH_2C_6H_4O$	−432	19.3	50.3	22.8	33.0
10	$Me_2NCH_2CPh_2O$	−462	16.1	50.1	27.6	32.6
11	$Ph_2P(S)S$	−246	20.7	51.3	31.0	31.7
12	*p*-*t*-Bu $C_6H_4C(O)O$	−416	18.3	50.5	25.7	35.8
13	Cl	−243	22.6	52.8	25.5	32.4
14	Br	−248	22.2	54.0	28.7	32.1
15	I	−396	22.1	53.7	33.1	30.5
16	$N(CH_2CMe_2O)_3SnOSiMe_2$- *p*-$C_6H_4SiMe_2O$	−313	18.3	50.2	18.2	31.5

Table 7. Parameters of Electrochemical Oxidation of Stannatranes 4, 8, 13, and 15 at a Platinum Disk Electrode

cmpd	solvent	E_p, V[a]	$E_p - E_{p/2}$, V	$\Delta E_p/\Delta\lg(v)$, mV	*n*	α[b]	$\Delta E_p/\Delta\lg(v)$ mV[c]	IP, eV
4	CH_3CN	1.47	0.171	40	0.94	0.3	23	5.569
4	CH_3CN/CH_2Cl_2	1.46	0.115	48	0.94	0.4	19	
4	CH_2Cl_2	1.33	0.127	43	0.97	0.4	17	
8	CH_3CN	1.41	0.119	25	1.40[c]	0.4	22	5.959
8	CH_3CN/CH_2Cl_2	1.41 (1.47)[d]	0.098	49	1.18	0.5	25	
8	CH_2Cl_2	1.40 (1.53)	0.082	58	1.03	0.6	26	
13	CH_2Cl_2	>2.2						7.338
15	CH_2Cl_2	>2.3						

[a]Peak potentials at v = 1 V/s. [b]Formal transfer coefficient, found from $(E_p - E_{p/2})/1.85 = RT/\alpha F$.[60] [c]Two peaks merged. [d]Second of two peaks.

ESI-MS spectra showing the dissociation of the axial substituent under the experimental conditions employed. For none of the 1-alkoxy or 1-aryloxy substituted derivatives **1**−**7** the molecule mass cluster $[M + H]^+$ is observed. In contrast to this, the ESI-MS spectra of 1-(*p*-methylbenzenethiolate) **8** and of 1-alkoxy or 1-aryloxy substituted derivatives **9** and **10** containing additional NR_2 (**9**, R = H; **10**, R = Me) donor groups show the mass clusters $[\mathbf{8} + H]^+$ (90%), $[\mathbf{9} + H]^+$ (70%) and $[\mathbf{10} + H]^+$ (92%), respectively. The ESI mass spectra of **11**, **12**, **14** and **15** also confirm their identity as well as monomeric structures in solution by showing mass clusters centered at m/z = 600.2, 528.3, 430.1, or 477.9 which are assigned to $[\mathbf{11} + H]^+$, $[\mathbf{12} + H]^+$, $[\mathbf{14} + H]^+$, and $[\mathbf{15} + H]^+$, respectively. Furthermore, the monomeric structure of **13** in solution was verified by osmometric molecular weight determination in chloroform.

Electrochemical Studies. To get an insight into the intramolecular electronic interactions in the new stannatranes, the electrochemical behavior of several compounds was considered. Depending on their solubility, cyclic voltammetry of compounds **4**, **8**, **13**, **15** was carried out in acetonitrile (AN), CH_2Cl_2 or in a binary mixture (AN/CH_2Cl_2, 1:1 v/v) containing Bu_4NPF_6 (0.1 M) as supporting salt.

dx.doi.org/10.1021/ic202179e | *Inorg. Chem.* 2012, 51, 1041−1056

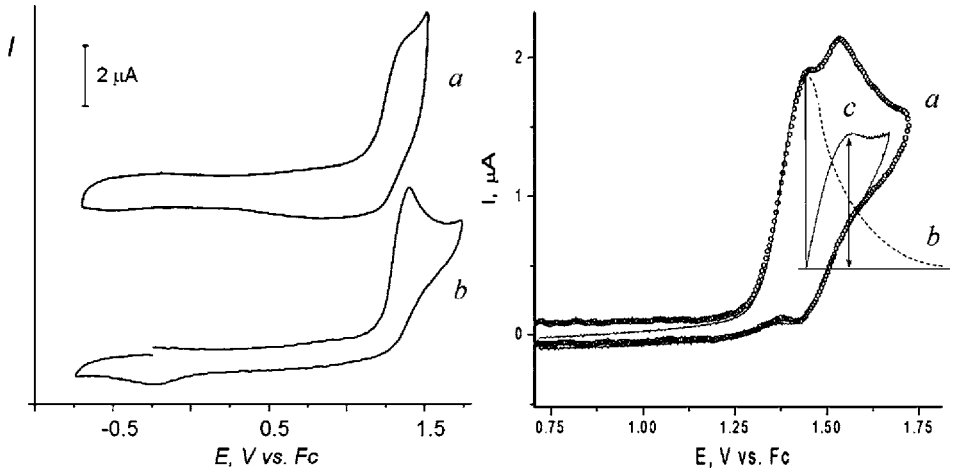

Figure 14. Cyclic voltammograms for the oxidation of stannatranes. Left: (a) − **4** and (b) − **8** (10^{-3} mol L^{-1}) in CH_3CN/0.1 M Bu_4NPF_6 at a Pt disk electrode; v = 5 V/s. Right: I–E curve of **8** (1.1×10^{-3} mol L^{-1}) in CH_2Cl_2/0.1 M Bu_4NPF_6 at a Pt disk electrode. (a) normal scan; (b) I–t curve after the hold at E_p^1. (c) diffusion limiting current of the second oxidation step. v = 0.5 V s^{-1}; T = 22 °C.

Contrary to silatranes[44,45] and germatranes,[46] the stannatranes **4** and **8** show distinct oxidation signals only at a Pt electrode. The limiting currents i_p of stannatranes **4** and **8** are both diffusion controlled ($i_p/v^{1/2}$ = const; $\lg(i_p)/\lg(v)$ = 0.45 and 0.46 for **4** and **8**, respectively) and, as was shown using $i_p/v^{1/2}$ ratio along with Cottrell slope from chronoamperometry at the same electrode,[47] the number of electrons transferred at this step is n = 1 (Table 7). Temperature dependence of $\lg(i_p^1)$ of **8** provides E_a = 2.46 kJ/mol (2.85 kJ/mol for second peak), corresponding to the activation energy of the diffusion flow of solvent. The peak half-widths $E_p - E_{p/2}$ of **4** and **8** are too large for simple one-electron reversible processes, supposedly because of the adsorption interactions or substantial structural reorganization accompanying electron transfer.

In a less polar solvent such as CH_2Cl_2, the oxidation of **8** proceeds via two steps (Figure 14), with the second one being reversible already at v = 0.5 V s^{-1}. With the vertex potential set before the onset of the second oxidation peak (E_v = 1.45 V), the first peak also starts showing cathodic counterpart (at v > 50 V/s). Thus, both oxidation signals arise from electrochemically reversible processes. The i–t curve with the hold at E_p^1 (Figure 14) allowed to subtract the diffusion limited current of the first peak i_p^1 (the baseline for the second peak[48] and to quantify the current of the second oxidation step, i_p^2. The latter was shown to have an electron stoichiometry of n = 0.4, caused by self-reactions involving cation radicals, as it was observed in the case of oxidation of Ar_2S or ArSM[49] with the HOMO localized on the ArS fragment. Thus, the similarity in the oxidation pattern of **8** and aryl sulfides suggests that the *p*-$CH_3C_6H_4S$ fragment in **8** is most probably the reaction site that accounts for the first oxidation peak. The E_p of compound **8** is about 150–200 mV higher than those of diaryl or arylalkyl sulfides,[50] due to the electron acceptor effect of the stannatranyl substituent. The possibility of oxidation of the stannatranyl moiety at E_p^2 should obviously be ruled out because not only the HOMO but also the lower lying HOMO−1 in **8** is mostly built of sulfur atom orbitals. Moreover, considering orbital energies (as IP = $-\varepsilon_{HOMO}$ in Koopman's approach, by B3LYP/LANL2DZ) of HOMO−1 in **8** (6.655 eV) and of SOMO in $\mathbf{8}^{+\bullet}$ (6.094 eV), it is more probable that a second electron withdrawal affects the cation radical, like in the case of aryl sulfides. In contrast to the trend in E_p^{ox} of diaryl and arylalkyl thioethers, which are easier to oxidize than parent ethers,[50] the order of E_p values for oxygen- and sulfur-containing stannatranyl derivatives is reversed (Table 7). This is supposedly because of stronger Sn–S versus Sn–O bonding and a stronger acceptor effect of the stannatranyl moiety on the E_p of **8** compared to the E_p of **4**.

The stannatranes **13** and **15** did not show any distinct oxidation peaks up to the media limits. As was pointed out by Broka et al.,[45] the chlorido-substituted silatrane $N(CH_2CH_2O)_3$-SiCl cannot be oxidized. No such data exist for the chlorido-substituted germatrane $N(CH_2CH_2O)_3GeCl$ but one can expect even higher E_p since germatranes are more difficult to oxidize than silatranes.[46,51] From a simple correlation of E_p with calculated IPs of the stannatranes **4**, **8**, and **13**, the oxidation potential of the chlorido-substituted derivative **13** should be above 2.3 V which corroborates the results of its voltammetry.

On the contrary, compound **13** shows a well-shaped reduction peak at E_p = −1.5 V; the reduction process results in elimination of Cl^- anions whose oxidation peak at ∼1 V is detected by voltammetry during the second cycle. The peak at −1.5 V falls into the range of reduction potentials of known chloridostannanes[52] and might have arisen from the dissociative reduction of Sn–Cl bond in **13**. Similarly, the oxidation peak of the iodide anion I^- appears after the reduction of **15**. This is in agreement with the conductivity measurements of **13** in CH_3CN/CH_2Cl_2 (50:50 v/v), which have only shown residual solvent conductance and no contribution from any ionic conductivity due to the possible Sn–Cl dissociation prior to the reduction. A practically identical conductivity curve was observed for the phenolato-substituted stannatrane **4**. Therefore the chlorido-substituted stannatrane **13**, just as **4**, remains a covalent compound in solution, at least in this media.

EPR-Spectroelectrochemistry. Since the oxidation of the phenolato-substituted stannatrane **4** shows partial reversibility (Figure 14), it was studied by real-time EPR-coupled electrochemistry. The solution of **4** (10^{-3} mol L^{-1}) in AN/0.1 M Bu_4NPF_6, initially ERP-silent, has shown the signal of paramagnetic species when the potential 1.23 V was applied (Figure 15).

The visible end-to-end span of the observed spectrum (Δ = 23–24 G) corresponds to the coupling constants from 2 sets of equivalent protons and to some contribution from $^{117/119}Sn$ nuclei. The g-factor (g = 2.0036) is slightly increased relative to that of pure organic radicals because of the interaction with

dx.doi.org/10.1021/ic202179e | Inorg. Chem. 2012, 51, 1041–1056

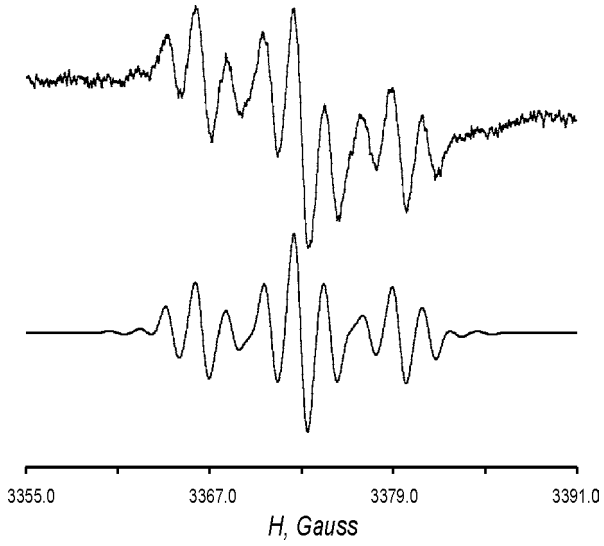

Figure 15. EPR spectrum from the oxidation of stannatrane **4** in AN/0.1 M Bu_4NPF_6 at a Pt microspiral electrode. Upper, experimental; lower, simulated using the parameters in the text. T = 233 K, E = 1.23 V.

oxygen and tin and falls into the range of the values for known phenoxyl radicals.[53,54] The triplet of triplets pattern with 1:2:1 intensities is rather straightforward and fits well with two pairs of practically equivalent protons (*o,o'*- and *m,m'*-) in the supposed phenoxyl species. Though the ends of the spectrum are not well enough resolved to allow extracting exact $Sn^{119/117}$ coupling constants, its symmetry permits to suppose two values aSn^{119} = 6.7 G and aSn^{117} = 7.4 G.

The set of 2H with the *hfc* constant of aH_o = 6.22 G can be substituted with two large proton *hfc* constants (aH_{o} = 6.27 G and $aH_{o'}$ = 6.03 G), assigned to two slightly different *ortho*-protons of the phenyl ring (see Figure 14). This substitution provides a better fitting but in any case, this difference is at the level of the (possible) contribution from the protons of the *t*-Bu group. Two *m*-protons account for a smaller constant, aH_m = 1.85 G (2H). It appears as there is no coupling with the atrane cage nitrogen atom or, if any, its contribution is very small. In general, the presence of d-metals often results in strong spin−orbital interactions[55] broadening the spectral lines and making it difficult to observe well resolved hyperfine structure. Thus the cation radical, hereafter referred to as CR, of stannatrane **4** has the spin distribution as an O-substituted *t*-Bu-phenoxy radical and not as a proper metallatrane, similarly to the cation radicals of germatranes in which the 1-substituent has lower own ionization potential than the atrane nitrogen atom.[51]

DFT Calculations. The geometry of the stannatranes **4**, **8**, and **13** and of their cation radicals was optimized using a combined treatment: primary adjustment was done at HF/6-311G level, and then the structure was optimized at DFT B3LYP/DGDZVP level, better accounting for long-term and delocalizing electronic interactions. The same level was used for NBO analysis and to check the optimized structures for the absence of imaginary vibrations.

The N−Sn distance is very little affected by electron withdrawal. It becomes slightly longer in $\mathbf{4}^{+\bullet}$, slightly shorter in $\mathbf{8}^{+\bullet}$ and remains practically unchanged in $\mathbf{13}^{+\bullet}$ (Table 8). Meanwhile, other geometrical parameters of these stannatranes show remarkable configurational change when forming the cation radical. Thus, for the neutral stannatrane **4**, the dihedral angle φ ($\angle C_{o\text{-}Ar}-C_{i\text{-}Ar}-O-Sn$) is 93.63°, while it becomes 3.81° in the cation radical (Figure 16) showing that the atrane moiety twists

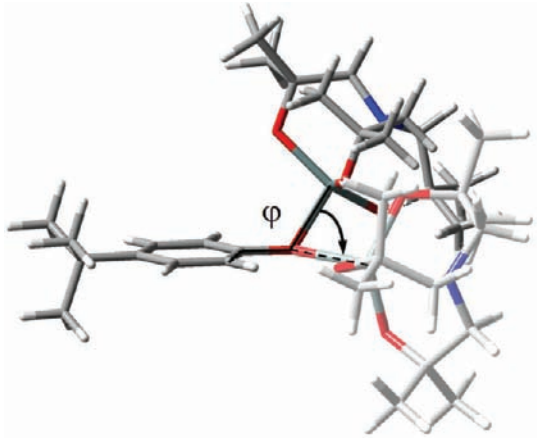

Figure 16. B3LYP/DGDZVP optimized geometry of stannatrane **4** and its cation radical (see text).

around the O−Sn bond by the right angle (55° for the couple $\mathbf{8}/\mathbf{8}^{+\bullet}$). The driving force of this remarkable twist is the interaction of p_z-orbitals of the O and S atoms with the π-systems of the aromatic fragments, destabilizing the HOMO in the neutral molecules and stabilizing the corresponding CRs. The stabilization of the phenoxy system in $\mathbf{4}^{+\bullet}$ is stronger than of the arylthio fragment in $\mathbf{8}^{+\bullet}$: while the couple $\mathbf{4}/\mathbf{4}^{+\bullet}$ clearly switches between two most stable − orthogonal and planar − forms (both corresponding to global minima on the energy surface), the bulkiness of the S atom and the poorer match in the size of overlapping orbitals in $\mathbf{8}^{+\bullet}$ force the latter to adopt a compromise half-eclipsed configuration. It implies that the nuclear frames of **4** and **8**, following the redistribution of the

Table 8. Selected Geometrical Parameters (Distances in Å, Angles in Degrees), Fermi Contact Terms (FCT, MHz), and NBO Charges for Stannatranes 4, 8, 13, and Their Cation Radicals from DFT B3LYP/DGDZVP Calculations

						N		Sn	
compd	l(Sn−N)	l(Sn−X)[a]	∠N−Sn−X	∠X−Sn−O[b]	∠O−Sn−O[b]	FCT	q(NBO)	FCT	q(NBO)
4	2.240	2.030	171.66	102.46 (89.07)	126.77 (101.43)		−0.348		1.296
$\mathbf{4}^{+\bullet}$	2.265	2.121	177.84	96.32 (98.93)	118.73	0.0000	−0.342	−0.3056	1.307
8	2.402	2.442	175.94	101.72	116.02		−0.326		1.171
$\mathbf{8}^{+\bullet}$	2.273	2.582	173.82	99.99 (91.72)	118.46	0.0003	−0.342	−2.6584	1.196
13	2.374	2.373	179.97	100.60	116.69		−0.327		1.195
$\mathbf{13}^{+\bullet}$	2.376	2.332	164.89	105.72 (90.45)	th126.34 (111.03)	0.7022	−0.327	104.5738	1.163

[a]X is first atom of the 1-substituent, as in Scheme 4. [b]for two Sn-symmetrical O_{eq} atoms, the value given in the parentheses is for the remaining nonsymmetrical O_{eq}.

dx.doi.org/10.1021/ic202179e | *Inorg. Chem.* 2012, 51, 1041−1056

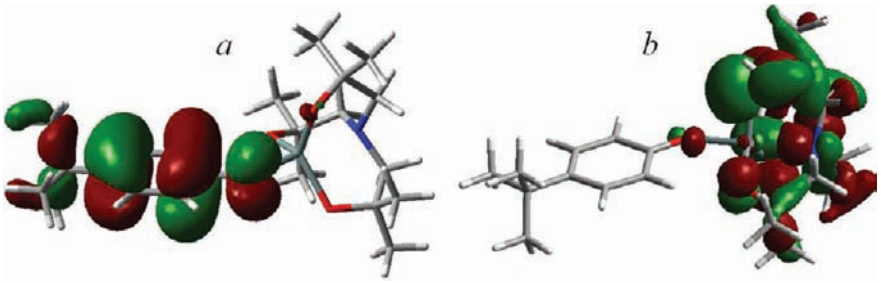

Figure 17. Unpaired electron density (SOMO) delocalization on the phenoxy fragment in the cation radical $4^{+\bullet}$ by B3LYP/DGDZVP (a), and doubly populated (SOMO−1) orbital (b) with small contribution of 3c−4e N−Sn−O bonding.

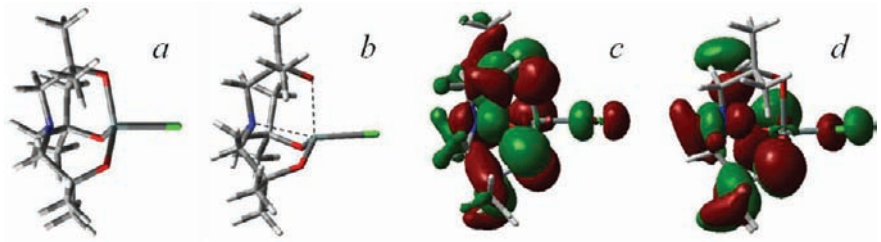

Figure 18. Geometry and FMOs for $13/13^{+\bullet}$ from B3LYP/DGDZVP optimization: (a) neutral, (b) cation radical, (c) HOMO of **13** and (d) SOMO of $13^{+\bullet}$. The contribution of intramolecular N−Sn−O (3c-4e) bonding is clearly seen, though with moderate orbital coefficients.

electron density upon oxidation (electrochemical electron transfer is adiabatic by its nature), exist in two fixed geometries: those of neutral and of the oxidized forms (**4** vs $4^{+\bullet}$ and **8** vs $8^{+\bullet}$). This fact precludes the formation of pure Nernstian reversible redox systems for these compounds which accounts for small apparent transfer coefficient α for **4** and **8** (Table 7). There is no contribution of the nitrogen atom to the spin−orbital interactions in $4^{+\bullet}$ since the 3c-4e system has lower energy than SOMO (Figure 17) and is doubly populated. The $4^{+\bullet}$ is thus a phenoxyl radical; it agrees very well with its EPR spectrum that has no characteristic pattern of a nitrogen-centered radical. Fermi contact couplings at the nitrogen and tin atoms (Table 8), and at the atoms of the phenoxy fragment, obtained from B3LYP/DGDZVP calculations, agree well with this feature. Contrary to CRs of germatranes, showing no unpaired spin density on the germanium atom and no coupling with it,[56] the spectrum of the iodido-substituted stannatrane **15** shows the $^{117/119}$Sn satellites which is also consistent with the nonzero FCT on the Sn atom (Table 8).

Upon oxidation of the chlorido-substituted stannatrane **13**, the tin atom also undergoes substantial reorganization: instead of a trigonal bipyramid it adopts the configuration of the pyramid with a rhombic base, when one oxygen atom is at the apical position and the long diagonal of the base is formed by nitrogen and chlorine atoms (Figure 18); in general it resembles to Berry pseudorotation transition state. The calculated Sn−O_{eq} bond length is 1.994 Å in average, whereas the third Sn−O_{eq} distance (for which ∠Cl−Sn−O_{eq} = 90°) is 2.244 Å. The N−Sn−Cl angle being 180° in the neutral molecule is smaller by about 15°, bringing closer the nitrogen and chlorine atoms (Table 8).

The structure of the HOMO of the chlorido-substituted stannatrane **13** is rather complex (Figure 18). Contrary to the HOMO's of lighter metallatranes (M = Si, Ge) the 3c-4e bonding system of which involves the easiest to ionize orbital (n-electrons of N),[46,56,57] the HOMO of **13** only contains it to a small extent (at least, at the B3LYP/DGDZVP theory level) suggesting that upon electron withdrawal, the whole orbital system involved must be very perturbed with no possibility of delocalizing stabilization of the cation radical. The spin-bearing orbital in $13^{+\bullet}$ is mainly localized on the tin atom (sf. Table 8), and is neither sterically shielded nor involved into conjugation as in germatranes.[46,56] On this reason it is probably much more difficult to observe this species in solution, since it is closer to R_4Sn or R_5Sn radicals[58] than to known CRs of sila- or germatranes with N-centered spin-carrying orbitals.[46,56,57] The importance of surrounding Sn O_{eq}-atoms in the HOMO suggests a strongly perturbed Sn environment upon electron removal leaving few chances for observing such CR under conventional conditions. It is then rather questionable whether it is possible to observe these species in solution, above the freezing point of common electrochemical solvents. Also, **13** has high value of the ionization potential (Table 7) which, using the approximate E_p − IP correlation, leads to the E_p of about 2.4−2.6 V, meaning that the oxidation of this stannatrane could not be observed under the conditions employed. However, these estimations are based on the gas phase data and bonds polarization in the solution might lower the actual oxidation potential, so a broad shoulder observed at ∼2.2−2.3 V for **13** and **15** in CH_2Cl_2 might actually stem from this oxidation. In any case, high oxidation potential of **13** and **15** excludes the use of spin traps because many of them undergo oxidation much before these potentials.[59]

CONCLUSION

In this manuscript we have demonstrated the high potential of the *t*-butoxido-substituted stannatrane $N(CH_2CMe_2O)_3SnO$-*t*-Bu (**1**) for the synthesis, in mostly acid−base-type reactions, of a great variety of novel inorganic stannatranes of the type $N(CH_2CMe_2O)_3SnX$ (X = OR, SR, $OSiMe_2C_6H_4SiMe_2O$Sn-$(OCMe_2CH_2)_3N$, OC(O)R, $SP(S)Ph_2$, halogen). In fact, compound **1** is a tin tetraalkoxide the cage-type structure including intramolecular N→Sn interaction of which induces high reactivity of the axial Sn−O bond only. Consequently, compound **1** might

dx.doi.org/10.1021/ic202179e | *Inorg. Chem.* 2012, 51, 1041−1056

be an ideal candidate for the controlled functionalization of acidic surfaces. In this sense, an even higher reactivity is to be expected for amino-substituted stannatranes of the type $N(CH_2CMe_2O)_3SnNR_2$ (R = H, alkyl, aryl) the synthesis of which is envisaged. Electrochemical measurements show that anodic oxidation of the stannatranes **4** and **8** occurs via electrochemically *reversible* electron transfer resulting in corresponding cation radicals (CRs) detected by CV and real-time EPR spectroelectrochemistry. The own oxidation potential of the X-Ar substituent in these compounds is lower than that of the stannatranyl moiety, so **4** and **8** follow the oxidation pattern and form the CRs of the corresponding aromatic derivatives substituted with a stannatranyl group.

■ ASSOCIATED CONTENT

Supporting Information

CIF file, figures showing molecular structures, ^{119}Sn CP MAS NMR, powder X-ray diffraction, and ^{13}C CP MAS NMR, and tables showing crystal data and structure refinement. This material is available free of charge via the Internet at http://pubs.acs.org.

■ AUTHOR INFORMATION

Corresponding Author

*klaus.jurkschat@tu-dortmund.de.

■ REFERENCES

(1) Baltkais, N. J.; Voronkov, M. G.; Zelchan, G. I. *Izv. AN Latv. SSR, ser. khim.* **1964**, *2*, 102.
(2) Martinez, A.; Robert, V.; Gornitzka, H.; Dutasta, J.-P. *Chem.—Eur. J.* **2010**, *16*, 520−527.
(3) Evgeniou, E. M.; Pergantis, S. A.; Leontidis, E.; Keramidas, A. D. *Inorg. Chem.* **2005**, *44*, 7511−7522.
(4) Tasaka, M.; Hirotsu, M.; Kojima, M.; Utsuno, S.; Yoshikawa, Y. *Inorg. Chem.* **1996**, *35*, 6981−6986.
(5) Singh, A.; Mehrotra, R. C. *Coord. Chem. Rev.* **2004**, *248*, 101−118.
(6) Karlov, S. S.; Tyurin, D. A.; Zabalov, M. V.; Churakov, A. V.; Zaitseva, G. S. *J. Mol. Struct. (THEOCHEM)* **2005**, *724*, 31−37.
(7) Phukan, A. K.; Guha, A. K. *Inorg. Chem.* **2010**, *49*, 9884−9890.
(8) Phukan, A. K.; Guha, A. K. *Inorg. Chem.* **2011**, *50*, 1361−1367.
(9) Verkade, J. G. *Coord. Chem. Rev.* **1994**, *137*, 233−295.
(10) Karlov, S. S.; Zaitseva, G. S. *Chem. Het. Comp.* **2001**, *37*, 1325−1357.
(11) Puri, J. K.; Singh, R.; Chahal, V. K. *Chem. Soc. Rev.* **2011**, *40*, 1791−1840.
(12) Ovchinnikov, Y.; Struchkov, Y.; Baryshok, V.; Voronkov, M. *J. Struct. Chem.* **1994**, *35*, 750−753.
(13) Tzschach, A.; Pönicke, K. *Z. Anorg. Allg. Chem.* **1975**, *413*, 136−142.
(14) Jurkschat, K.; Mügge, C.; Tzschach, A.; Zschunke, A.; Engelhardt, G.; Lippmaa, E.; Mägi, M.; Larin, M. F.; Pestunovich, V. A.; Voronkov, M. G. *J. Organomet. Chem.* **1979**, *171*, 301−308.
(15) Swisher, R. G.; Day, R. O.; Holmes, R. R. *Inorg. Chem.* **1983**, *22*, 3692−3695.
(16) Tzschach, A.; Jurkschat, K. *Comm. Inorg. Chem.* **1983**, *3*, 35−50.
(17) Dakternieks, D.; Dyson, G.; Jurkschat, K.; Tozer, R.; Tiekink, E. R. T. *J. Organomet. Chem.* **1993**, *458*, 29−38.
(18) Li, J.; Liao, R.-A.; Xie, Q.-L. *Prog. Nat. Sci.* **1994**, *4*, 68−72.
(19) Ravenscroft, M. D.; Roberts, R. M. G. *J. Organomet. Chem.* **1986**, *312*, 45−52.
(20) Li, J.; Tang, Y.-J.; Liu, H.; Dong, S.-P.; Xie, Q.-L. *Gaodeng Xuexiao Huaxue Xuebao* **1998**, *19*, 1074−1077.
(21) Kolosova, N. D. Z., N. N.; Shriro, V. S.; Kocheskov, K. A.; Barminova, N. P. Patent SU 643508 A1 19790125, 1979.
(22) E. F. Rickard, C.; R. Roper, W.; J. Woodman, T.; James Wright, L. *Chem. Commun.* **1999**, 837−838.
(23) Clark, A. M.; Rickard, C. E. F.; Roper, W. R.; Woodman, T. J.; Wright, L. J. *Organometallics* **2000**, *19*, 1766−1774.
(24) Ilyukhin, A. B.; Davidovich, R. L.; Logvinova, V. B. *Russ. J. Inorg. Chem.* **1999**, *44*, 1833−1836.
(25) Zöller, T.; Iovkova-Berends, L.; Berends, T.; Dietz, C.; Bradtmöller, G.; Jurkschat, K. *Inorg. Chem.* **2011**, *50*, 8645−8653.
(26) Zöller, T.; Iovkova-Berends, L.; Dietz, C.; Berends, T.; Jurkschat, K. *Chem.—Eur. J.* **2011**, *17*, 2361−2364.
(27) Berends, T.; Iovkova, L.; Bradtmöller, G.; Oppel, I.; Schürmann, M.; Jurkschat, K. *Z. Anorg. Allg. Chem.* **2009**, *635*, 369−374.
(28) Krause, J.; Richter, S.; Lindner, S.; Schmidt, A.; Jurkschat, K.; Schürmann, M.; Bradtmöller, G.; DE 10 2008 021 980 A1: 2009.
(29) Amarego, W. L. F.; Chai, C. L. L. *Purification of Laboratory Chemicals*, 5th ed.; Butterworth-Heinemann: Oxford, U.K., 2003.
(30) Mun, S.-d.; Lee, J.; Kim, S. H.; Hong, Y.; Ko, Y.-h.; Shin, Y. K.; Lim, J. H.; Hong, C. S.; Do, Y.; Kim, Y. *J. Organomet. Chem.* **2007**, *692*, 3519−3525.
(31) Merker, R. L.; Scott, M. J. *J. Polym. Sci., Part A* **1964**, *2*, 15−29.
(32) Sieber, F.; W., P. Jr.; Toker, J. D.; Wentworth, A. D.; Metz, W. A.; Reed, N. N.; Janda, K. D. *J. Org. Chem.* **1999**, *64*, 5188−5192.
(33) Sheldrick, G. M. *Acta Crystallogr. A* **2008**, *64*, 112.
(34) Spek, A. L. *Acta Crystallogr.* **2009**, *D65*, 148.
(35) Mann, C. K.; Barnes, K. K. *Electrochemical Reactions in Nonaqueous Systems*; Marcel Dekker Inc.: New York, 1970.
(36) Zeitouny, J.; Jouikov, V. *Phys. Chem. Chem. Phys.* **2009**, *11*, 7161−7170.
(37) *WINEPR SimFonia*, version 1.25; Bruker Analytische Messtechnik GmbH, Karlsruhe, 1994−1996.
(38) Frisch, M. J.; Trucks, G. W.; Schlegel, H. B.; Scuseria, E.; Robb, M. A.; Cheeseman, J. R.; Montgomery Jr., J. A.; Vreven, T.; Kudin, K. N.; Burant, J. C.; Millam, J. M.; Iyengar, S. S.; Tomasi, J.; Barone, V.; Mennucci, B.; Cossi, M.; Scalmani, G.; Rega, N.; Petersson, G. A.; Nakatsuji, H.; Hada, M.; Ehara, M.; Toyota, K.; Fukuda, R.; Hasegawa, J.; Ishida, M.; Nakajima, T.; Honda, Y.; Kitao, O.; Nakai, H.; Klene, M.; Li, X.; Knox, J. E.; Hratchian, H. P.; Cross, J. B.; Adamo, C.; Jaramillo, J.; Gomperts, R.; Stratmann, R. E.; Yazyev, O.; Austin, A. J.; Cammi, R.; Pomelli, C.; Ochterski, J. W.; Ayala, P. Y.; Morokuma, K.; Voth, G. A.; Salvador, P.; Dannenberg, J. J.; Zakrzewski, V. G.; Dapprich, S.; Daniels, A. D.; Strain, M. C.; Farkas, O.; Malick, D. K.; Rabuck, A. D.; Raghavachari, K.; Foresman, J. B.; Ortiz, J. V.; Cui, Q.; Baboul, A. G.; Clifford, S.; Cioslowski, J.; Stefanov, B. B.; Liu, G.; Liashenko, A.; Piskorz, P.; Komaromi, I.; Martin, R. L.; Fox, D. J.; Keith, T.; Al-Laham, M. A.; Peng, C. Y.; Nanayakkara, A.; Challacombe, M.; Gill, P. M. W.; Johnson, B.; Chen, W.; Wong, M. W.; Gonzalez, C.; Pople, J. A. *Gaussian 03*, revision B. 01; Gaussian, Inc.: Pittsburgh, PA, 2003.
(39) Mun, S.-d.; Kim, S. H.; Lee, J.; Kim, H.-J.; Do, Y.; Kim, Y. *Polyhedron* **2010**, *29*, 379−383.
(40) Kolb, U.; Draeger, M.; Dargatz, M.; Jurkschat, K. *Organometallics* **1995**, *14*, 2827−2834.
(41) Caruso, J.; Alam, T. M.; Hampden-Smith, M. J.; Rheingold, A. L.; Yap, G. A. P. *J. Chem. Soc., Dalton Trans.* **1996**, 2659−2664.
(42) Hampden-Smith, M. J.; Wark, T. A.; Rheingold, A.; Huffman, J. C. *Can. J. Chem.* **1991**, *69*, 121−129.
(43) Burke, J. J.; Lauterbur, P. C. *J. Am. Chem. Soc.* **1961**, *83*, 326−331.
(44) Broka, K. G., V.; Stradins, J.; Zelcans, G. *Zhurn. Obsch. Khim.* **1991**, *61*, 1374−1378.
(45) Broka, K.; Stradins, J.; Glezer, V.; Zelcans, G.; Lukevics, E. *J. Electroanal. Chem.* **1993**, *351*, 199−206.
(46) Soualmi, S.; Ignatovich, L.; Lukevics, E.; Ourari, A.; Jouikov, V. *J. Organomet. Chem.* **2008**, *693*, 1346−1352.
(47) Malachesky, P. A. *Anal. Chem.* **1969**, *41*, 1493−1494.
(48) Bard, A. J.; Faulkner, L. R. *Electrochemical Methods: Fundamental and Applications*, 2nd ed.; John Wiley & Sons: New York, 2001.
(49) Wendt, H.; Hoffelner, H. *Electrochim. Acta* **1983**, *28*, 1465−1472.

(50) Jouikov, V.; Simonet, J. In *Encyclopedia of Electrochemistry*; Bard, A., Stratman, M., Shaefer, H., Eds.; Wiley-VCH: New York, 2004; Vol. *8*, pp 235−276.
(51) Soualmi, S.; Ignatovich, L.; Lukevics, E.; Ourari, A.; Jouikov, V. *ECS Trans.* **2008**, *13*, 63−69.
(52) Markusova, K.; Kladekova, D.; Zezula, I. *Chemicke Zvesti* **1980**, *34*, 726−39.
(53) Weiner, S. A. *J. Am. Chem. Soc.* **1972**, *94*, 581−584.
(54) Pokhodenko, V. D.; Kalibabchuk, N. N. *Teor. i Eksperim. Khim.* **1970**, *6*, 124−128.
(55) Gerson, W. H. *Electron Spin Resonance Spectroscopy of Organic Radicals*; Wiley-VCH: Weinheim, Germany, 2003.
(56) Soualmi, S.; Ignatovich, L.; Jouikov, V. *Appl. Organometal. Chem.* **2010**, *24*, 865−861.
(57) Jouikov, V. *ECS Trans.* **2010**, *28*, 5−16.
(58) Iley, J. In *The Chemistry of Organic Germanium, Tin and Lead Compounds*; Patai, S., Ed.; John Wiley & Sons: New York, 1995, p 267−290.
(59) McIntire, G. L.; Blount, H. N.; Stronks, H. J.; Shetty, R. V.; Janzen, E. G. *J. Phys. Chem.* **1980**, *84*, 916−921.
(60) Andrieux, C. P.; Saveant, J. M. In *Investigations of Rates and Mechanisms of Reactions*; Bernasconi, C. F., Ed.; Wiley-VCH: New York, 1986.